UNIVERSITI TEKNOLOGI MARA

MATHEMATICAL MODELLING OF POWELL-EYRING HYBRID NANOFLUID FLOW OVER A FLAT PLATE WITH THERMAL RADIATION, MAGNETOHYDRODYNAMICS, JOULE HEATING, AND NEWTONIAN HEATING EFFECTS

NUR ARIF HUSAINI BIN NORWAZA

MSc

December 2025

UNIVERSITI TEKNOLOGI MARA

MATHEMATICAL MODELLING OF POWELL-EYRING HYBRID NANOFLUID FLOW OVER A FLAT PLATE WITH THERMAL RADIATION, MAGNETOHYDRODYNAMICS, JOULE HEATING, AND NEWTONIAN HEATING EFFECTS

NUR ARIF HUSAINI BIN NORWAZA

Thesis submitted in fulfilment
of the requirements for the degree of
Master of Science (Mathematics)

Faculty of Computer and Mathematical Sciences

December 2025

CONFIRMATION BY PANEL OF EXAMINERS

I certify that a Panel of Examiners has met on 31 December 2025 to conduct the final examination of Nur Arif Husaini Bin Norwaza on his Masters of Science thesis entitled "Mathematical Modelling of Powell-Eyring Hybrid Nanofluid Flow over a Flat Plate with Thermal Radiation, Magnetohydrodynamics, Joule Heating, and Newtonian Heating Effects" in accordance with Universiti Teknologi MARA Act 1976 (Akta 173). The Panel of Examiner recommends that the student be awarded the relevant degree. The Panel of Examiners was as follows:

Ahmad Sazali Hamzah, PhD
Professor
Faculty of Applied Sciences
Universiti Teknologi MARA
(Chairman)

Mohammad Nawawi Seroji, PhD
Associate Professor
College of Engineering
Universiti Teknologi MARA
(Internal Examiner)

Mohd Zuli Jaafar, PhD
Senior Lecturer
Faculty of Applied Sciences
University of Bristol
(External Examiner)

PROF IR DR ZUHAINA HAJI ZAKARIA
Dean
Institute of Postgraduates Studies
Universiti Teknologi MARA

Date: 17 July 2024

AUTHOR'S DECLARATION

I declare that the work in this thesis was carried out in accordance with the regulations of Universiti Teknologi MARA. It is original and is the results of my own work, unless otherwise indicated or acknowledged as referenced work. This thesis has not been submitted to any other academic institution or non-academic institution for any degree or qualification.

I, hereby, acknowledge that I have been supplied with the Academic Rules and Regulations for Post Graduate, Universiti Teknologi MARA, regulating the conduct of my study and research.

Name of Student	:	NUR ARIF HUSAINI NORWAZA
Student ID. No.	:	2025763013
Programme	:	Master of Science (Mathematics) - CDCS752
Faculty	:	Faculty of Computer and Mathematical Sciences
Thesis Title	:	Mathematical Modelling of Powell-Eyring Hybrid Nanofluid Flow over a Flat Plate with Thermal Radiation, Magnetohydrodynamics, Joule Heating, and Newtonian Heating Effects
Signature of Student	:	……..
Date	:	December 2025

ABSTRACT

Hybrid nanofluids have gained increasing attention for their enhanced heat transfer capabilities compared to traditional fluids, especially in energy systems like solar collectors. Many studies agree that the size, shape, and material of nanoparticles play a significant role in determining how well these fluids perform thermally. However, when these nanofluids exhibit non-Newtonian behaviour, such as shear-thinning-and are exposed to complex influences like magnetic fields, surface roughness, and thermal radiation, their behaviour becomes much harder to predict. In particular, the Powell-Eyring model, which is well-suited for describing non-Newtonian fluids, has not been widely applied to hybrid nanofluid flows. There is still debate in the research community over which nanoparticle combinations and numerical methods provide the most reliable results, especially when modelling these fluids under conditions involving magnetohydrodynamics (MHD), and non-linear heat radiation. Some argue that added surface roughness improves heat transfer through turbulence, while others highlight the downside of increased frictional losses. Additionally, while numerical methods like bvp4c are commonly used, questions remain about their stability and accuracy in stiff or highly nonlinear systems. This research proposes to develop a mathematical model that captures the unsteady flow of a Powell-Eyring hybrid nanofluid over a flat surface, while considering effects such as magnetic fields, nonlinear thermal radiation, surface roughness and orientation, mixed convection, and suction or blowing. The resulting system of equations will be solved using a Block Backward Differentiation Formula (BBDF), and the results will be compared with those obtained from MATLAB's bvp5c solver to verify accuracy. The central hypothesis is that using a non-Newtonian model like Powell-Eyring, along with Block Backward Differentiation Formula (BBDF), will provide a clearer and more accurate understanding of how these nanofluids behave in real-world engineering conditions. It is anticipated that early results will show that certain combinations of nanoparticle types, magnetic field strengths, and surface effects can improve heat transfer significantly, making these models highly useful for future thermal system designs.

ACKNOWLEDGEMENT

Firstly, I wish to thank God for giving me the opportunity to embark on my PhD and for completing this long and challenging journey successfully. My gratitude and thanks go to my supervisor Dr. Iskandar Shah Bin Mohd Zawawi, internal co-supervisor Dr. Nur Syazana Binti Anuar.

Finally, this thesis is dedicated to the loving memory of my very dear late father and mother for the vision and determination to educate me. This piece of victory is dedicated to both of you. Alhamdulilah.

TABLE OF CONTENTS

LIST OF TABLES

LIST OF FIGURES

LIST OF PLATES

Plates **Title** **Page**

No table of figures entries found.

LIST OF SYMBOLS

Symbols

A	Number of PLS or PCA components in the model and the number of selected latent variable in the model
a	Number of the PLS or PCA component
b	PLS regression coefficient
b	Number of blocks (b=1,2,3.....,K)
C	Coarse APM block
$\boldsymbol{C}_p$	Pooled covariance matrix for the two classes
$\boldsymbol{C}_g$	Covariance matrix for class g

LIST OF ABBREVIATIONS

Abbreviations

PCA	Principal Component Analysis

LIST OF NOMENCLATURE

Nomenclatures

A	Amplitude Ratio, (No Units)
C	Centroid of pipe, inches

CHAPTER 1
INTRODUCTION

1.1 Research Background

1.2 Heat Transfer

Heat is a process of energy transfer from one system to another (Rennie & Law, 2019). As it is a transient phenomenon, it can only be identified as it crossed a boundary between multiple systems that have different temperature to achieve equilibrium (Escudier & Atkins, 2019).

From a mathematical perspective, heat Q is understood as a manifestation of internal energy where in a medium with specific heat capacity c, density ρ, at temperature T, reside in a region R, $Q = \iiint_R \rho c T \, dV$. In that it is energy, with the unit joule J. Here, heat is defined as a manifestation of internal energy distributed throughout a medium.(*The Concise Oxford Dictionary of Mathematics*, 2021). Heat here is framed as an internal state function. The region R must be well defined, and the variables must be sufficiently continuous. Since the thermal equilibrium assumption need to be implemented, each differential volume element must be small enough to assume a uniform temperature. Mass density ρ relates spatial volume to matter content, specific heat capacity c encodes the proportionality between temperature and internal energy, temperature T represent the state variable capturing thermal intensity, and spatial domain R is bounded region within which the energy is considered. This formulation provides a bridge between microscopic thermodynamics and macroscopic energy accounting.

Internal energy U is defined as the total of kinetic energy of the atoms and molecules in a system and the potential energy of their mutual interactions. It is not energy of the whole system itself, hence doesn't include nuclear and inter-atomic/extra-molecular energies. Absolute value of the internal energy can't be measured directly. The focus for this subject is on the change of the energy ΔU (Rennie & Law, 2019).

Thermodynamics discussion requires a clear distinction between the term heat Q and internal energy U. According to the first law of thermodynamics, they relate within a system by the definition of a change in internal energy $\Delta U = Q - W$ where Q is energy interaction as heat occurring into the system and W is work done by the system on its surroundings. Heat is a path-dependent process and not a state function. An accurate approach to describe heat is in a standard molar (with unit kJ mol^{-1}) enthalpy change for the process under consideration. (Rennie & Law, 2019). The analogy is like balance in bank account (internal energy), deposit (heat), and withdrawal for bill payment (work done).

The temperature T(x,t) in a uniform solid medium, as governed by the heat equation, satisfies the parabolic partial differential equation $\frac{\partial T}{\partial t} = k\frac{\partial^2 T}{\partial x^2}$, where k represents the thermal diffusivity of the medium (*The Concise Oxford Dictionary of Mathematics*, 2021). This is a reduced form of conservative of energy law under a specific assumption of homogeneity (the quality or state of being all the same or all of the same kind), no internal heat generation, and constant thermal diffusivity k. This is only applicable for heat transfer that only occur via conduction. The validity an dintegrity of this heat equation depends on the invariants of Faurier's Law (heat flux is propotional to the negative gradient of temperature, $q = -k\nabla T$), energy conservation, and linearity (nonlinear cases like turbulent flows, radiation dominance will break the model). The spatial Laplacian $\frac{\partial^2 T}{\partial x^2}$ encodes spatial curvature of temperature, determining how heat "flows" from hotter to colder regions with its neighbouring environment. This provides a predictive model for how heat diffuses through solids. The structure shows that thermal evolution is irreversible and dissipative, which describe the Second Law of Thermodynamics

Physically, heat transfer is the transfer of energy between multiple systems because of difference in temperature (Rennie & Law, 2019). In the sense of mechanical engineering, heat transfer (also known as heat transport, heat transmission, and heat flow) is the transport of energy within or between object or fluid. There are 3 basic modes of the transportation: conduction, convection, and radiation (Escudier & Atkins, 2019).

In conclusion, heat transfer is the process by which energy moves across system boundaries due to temperature differences, acting as a path-dependent interaction that alters a system's internal energy, occurring only when crossing between systems and manifested through conduction, convection, or radiation.

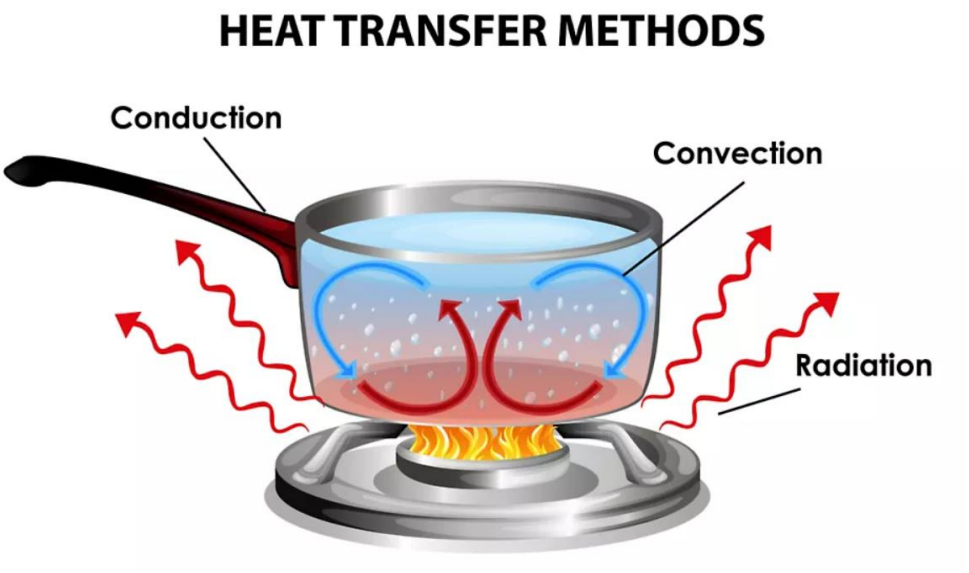

Figure 1: Heat transfer methods

1.2.1 Thermal Radiation

Radiation is energy travelling in the form of electromagnetic waves or photons (Rennie & Law, 2019).

1.2.2 Thermal Convection

Convection is process by which heat is transferred through the fluid itself. Natural convection is defined by the movement due to gravity; the hot part of the fluid expands, becomes less dense, and is displaced by the colder denser part of the fluid as this drops below it. This is the process that occurs in most domestic hot water. In some modern systems, where small-bore pipes are used or it is inconvenient to place the cylinder above the boiler, the circulation between boiler and hot-water cylinder relies

upon a pump. This is an example of forced convection, where hot fluid is transferred from one region to another by a pump or fan (Rennie & Law, 2019).

1.2.3 Thermal Conduction

Thermal conduction is the transmission of heat through a substance. In gases and most liquids, the energy is transmitted mainly by collisions between atoms and molecules with those possessing lower kinetic energy. In solid and liquid metals, heat conduction is predominantly by migration of fast-moving electrons, followed by collisions between these electrons and ions. In solid insulators the absence of free electrons restrict heat transfer to the vibrations of atoms and molecules within crystal lattices (Rennie & Law, 2019).

1.3 Hybrid Nanofluid

There are 2 states of motion studied in fluid mechanics which is statics and dynamics. Fluid statics is concerned with forces and pressures applied on idle liquids and gases while fluid dynamics study this condition on the fluid at motions (hydrodynamics for liquids, aerodynamics for gases)(Rennie & Law, 2019).

When a fluid flowing in medium with dimensions below 100nm, it is called nanofluidic, while nanofluid represent a colloidal suspension of nanoparticles in a base liquid (Escudier & Atkins, 2019). It is widely proven that nanofluids significantly improve thermal conductivity performance. Earlier studies shows that this is the case due to the improvement in heat transmission capabilities.

This interest cause researchers to further the study on this matter with the exploration on dispersing multiple types of nanoparticles, hence the creation of “hybrid nanofluid”. The unique properties of different nanoparticles interact synergistically, enhancing heat transfer performance by complementing each other's functions and compensating for individual limitations (Jusoh et al., 2024; Zainal et al., 2024). As hybrid composite is a composite reinforced by two or more variety of filament (Escudier & Atkins, 2019), hybrid nanofluid is saturation of more than one type of nanofluid. A single nanofluid is called mono nanofluid, while hybrid nanofluid could be ternary

(trihybrid) nanofluid or beyond, even though it usually being used to refer to binary nanofluid up to this date.

In conclusion, hybrid nanofluid is a multiphase fluid formed by dispersing two or more types of nanoparticles into a base liquid at the nanoscale, resulting in a synergistic colloidal medium whose enhanced thermal performance arises from the combined interaction of distinct particle properties, thereby improving energy interaction under fluid motion.

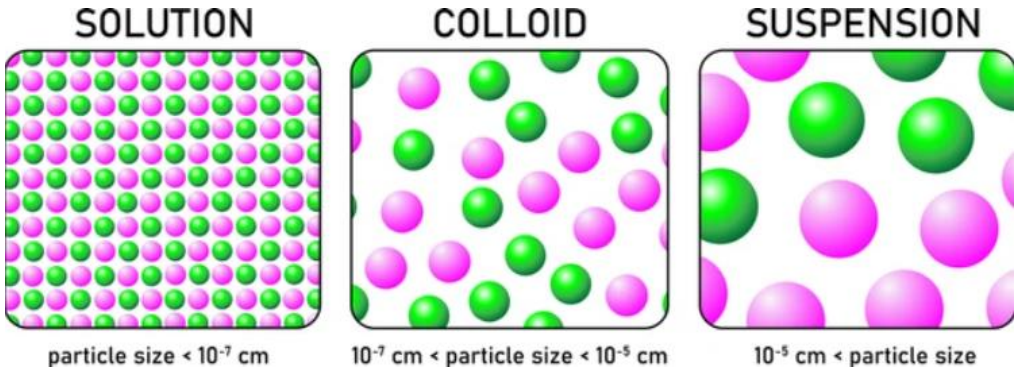

Figure 2: Colloidal Suspension of Hybrid Nanoparticles

1.4 Non-Newtonian Fluid

A Newtonian fluid is characterized by a linear relationship between shear stress and the velocity gradient, $\frac{F}{A} = \mu \frac{v}{d}$ where μ is the constant of proportionality (Newtonian viscosity). Hence, A non-Newtonian fluid is a fluid in which the relationship between shear stress and the velocity gradient does not consistently obey the linear model defined by Newton's law of viscosity. The viscosity is not constant and may vary with shear rate, time, or stress conditions. This type of fluid could exhibit increase in viscosity as the velocity gradient increases (dilatant during phenomenal dilatancy) like in some pastes and suspensions. There is no general theory has been developed to comprehensively describe them. However, it is common for non-Newtonian fluid to exhibit thixotropy where the viscosity depends on both velocity gradients and the time for which it has been applied (The faster a thixotropic liquid move, the less viscous it becomes) (Law & Rennie, 2020; Rennie & Law, 2019). Non-Newtonian fluid usually involving multiple combination of effects such as dependence of apparent viscosity

(effective viscosity, μ) on shear rate ($\dot{\gamma}$), normal stress (τ) in shear flow, time dependency, and memory effects (Escudier & Atkins, 2019). Because of these many kinds of rheological features different dependencies relational profile for different type and condition of non-Newtonian fluid, the behaviour for any non-Newtonian fluid can only be describes by using constitutive equations, an algebraic and numerical relation for the dependencies such as Hooke's Law, Newton's Viscosity Law, Fourier's Law, Fick's Law, and etc (Aminuddin, 2024; Escudier & Atkins, 2019).

One of the models used to study the behaviour of non-Newtonian fluid flow is the Powell–Eyring model. This model is known for its realistic consideration of shear-thinning behaviour in fluid viscosity. The constitutive equation is given by:

$$T = \mu \nabla V + \frac{1}{\beta} \sinh^{-1}\left(\frac{1}{c} \nabla V\right)$$

where μ is the dynamic viscosity, β and c are the characteristics of the Powell -Eyring model (Zaman et al., 2013), the material constants characterizing non-Newtonian response. The Powell-Eyring model is a constitutive equation describing the stress-strain relationship in non-Newtonian fluids that exhibits shear-thinning (viscosity decreases with shear rate). It is the extension of Newton's law of viscosity ($T = \mu V$, which assumes constant viscosity regardless of shear rate). The modal is applicable for fluid that exhibits shear-thinning behaviour, stable temperature and pressure, and the deformation rate is within a range where the inverse hyperbolic sine term realistically approximates molecular behaviour (if the deformation rate too low, the fluid looks nearly Newtonian with linear stress-strain, and if it too high, the molecular behavior deviates beyond the validity of the Powell-Eyring model). To maintain the coherence of this model, the positivity of viscosity must hold, the material constants β and c must be realistics and calibrated experimentally, dimensional consistency, and the asymptotic limits (small and large shear rates) must agree with realistics observed fluid behavior. The dynamic viscosity μ is for the baseline of Newtonian response, shear rate V is the driving variable controlling the stress, the material constants β and c shape the degree and onset of shear-thinning, the non-linear adjustment term

$\frac{1}{\beta}\sinh^{-1}\left(\frac{1}{c}\nabla V\right)$ capture the departure from Newtonian linearity. This formulation describe a smooth transition between Newtonian behavior at low shear rates and strong non-Newtonian effects at high shear rates. If $\mu = 0$, only the nonlinear term remains; at very low shear, the model loses Newtonian recovery and fails. If β and c are mis-specified, predictions deviate drastically, especially in high-shear conditions.

In conclusion, a non-Newtonian hybrid nanofluid is a colloidal suspension of two or more distinct nanoparticles in a base fluid that exhibits spacetime-dependent or complex rheological behaviour such as shear-thinning, shear-thickening, or thixotropy deviating from Newton's law of viscosity. One of its key advantages is leveraging synergistic nanoparticle interactions to enhance thermal performance beyond that of mono nanofluids.

1.5 Boundary Layer

Boundary layer is a thin layer of fluid formed on the surface relative to which the fluid is flowing. When a fluid touches a surface during the flow, it causes an adhesion between the molecules of the fluid closest to the solid surface result to those molecules of the fluid to be relatively stationary. The velocity of the fluid reduces from the value of free flow, U_∞ approaches to 0 relative to its closeness to the solid surface because of the attraction force between the molecules is stronger here. This is what we called as no-slip boundary condition, an accurate assumption for approximation for macroscopic flow, but not accurate at molecular scale. The opposition assumption for this boundary slip is slip boundary condition. This is the phenomena where viscosity in the bulk and at the surface of the liquid to be different (Asshaari & Md Jedi, 2022; Rennie & Law, 2019). The effect of viscosity is a key here. The Navier-Stokes equations are used to analyse the boundary layer, where the height of the layer approached to 0, and the effect of viscosity are approached to 0 at outside of the boundary layer (*The Concise Oxford Dictionary of Mathematics*, 2021).

In a field of mechanical engineering, there are two main topics on the boundary layer, the hydrodynamic boundary layer (velocity) and the thermal boundary layer (temperature). Hydrodynamic boundary layer is a developing region within a fluid that caused by the viscosity of the fluid when it flows over a surface. A stationary molecule of the fluid closest to the surface approaches to its free-stream value at the border of the boundary layer. Raynold number is used to identify the type of flow within the boundary layer whether it is laminar, transitional or turbulent. The thermal boundary layer is the thin region of a fluid near surface where heat transfer occurs due to a temperature difference between the surface and the free stream, resulting in a temperature gradient within the fluid (Escudier & Atkins, 2019). It is mentioned by Asshaari & Md Jedi (2022) that the temperature differences also occur due to the velocity of the fluid flow where the gap in temperature increase as the velocity of the fluid increase. This gap in temperature is also what we call thermal boundary layer. There is also research on the third kind of boundary layer which is concentration boundary layer (Asshaari & Md Jedi, 2022) where the boundary is defined by the difference in the concentration of the fluid.

In conclusion, boundary layer is the region of a fluid flow adjacent to a solid surface where the effects of viscosity are significant, resulting in steep gradients of physical properties such as velocity, temperature, or concentration, due to the no-slip condition or thermal interaction at the surface, regardless of the region's geometric thickness.

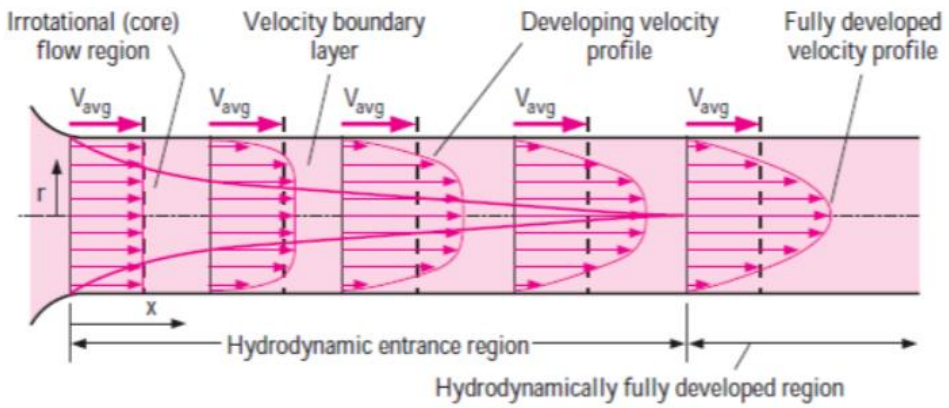

Figure 3: Boundary layer flow in pipe

1.6 Motivation for This Work

1.7 Problem Statement

Hybrid nanofluids (HNFs) are known to enhance thermal conductivity. However, most researchers adopt a narrowly focused scope, despite the wide range of non-Newtonian fluid behaviours that could be considered for specific applications. Very few studies couple Powell-Eyring shear-thinning rheology with the simultaneous action of magnetohydrodynamics, Joule heating, non-linear thermal radiation and Newtonian surface heating in a unified boundary-layer framework for application in solar collector device. Even the latest tri-hybrid investigations still exclude key loss mechanisms. It is required for a rigorously validated, integrated model that captures these concurrent effects over the receiver surfaces found in the renewable-energy hardware.

Runge-Kutta and MATLAB bvp4c are widely used, but their mesh adaptation deteriorates for strongly non-linear, stiff ODE systems that arise when MHD forces and viscous dissipation are large. Block Backward Differentiation Formulae (BBDF) offer better stability and have not been benchmarked against bvp5c for Powell-Eyring HNFs. Consequently, the community lacks solver reliability guidelines for collector-design calculations.

1.8 Research Objectives

1. To formulate mathematical models of Powell-Eyring hybrid nanofluid flow with thermal radiation over a flat plate, accounting for magnetohydrodynamics (MHD), Joule heating, and Newtonian heating effects for different surface orientation.
2. To transform the governing models into a system of ordinary differential equations (ODEs) through appropriate similarity variables.
3. To solve the resulting equations numerically using block backward differentiation formula (BBDF) and MATLAB's solver.
4. To analyse the impact of thermal radiation, MHD, Joule heating, and Newtonian heating on the behaviour of the fluid flow and heat transfer.

1.9 Research Question

1.10 Significance of Study

This research carries meaningful benefits across multiple areas of life. For society, it supports the global shift toward cleaner and more sustainable energy. By improving how we transfer and manage heat in solar energy systems, the study helps make renewable technologies like flat plate and parabolic trough solar collectors more efficient and practical for everyday use. This means better access to affordable and eco-friendly energy for households and communities, especially in regions with high solar potential.

In the world of academia, the study brings fresh insights by combining several advanced concepts like non-Newtonian fluid behaviour, hybrid nanofluids, and magnetic and thermal effects, into one unified mathematical model. Using the Powell-Eyring model and advanced numerical methods like the Block Backward

Differentiation Formula (BBDF), it opens new pathways for researchers to study complex heat flow systems more accurately. This contribution helps push the boundaries of applied mathematics and fluid dynamics research.

For government and policymakers, the research offers data and tools that can be used to set better design standards and performance expectations for renewable energy infrastructure. With more reliable modelling, solar systems can be built to perform better under real-world conditions, supporting national energy goals and long-term climate commitments.

From an industry point of view, especially in the energy and engineering sectors, the findings can guide manufacturers and designers in improving the performance of solar collectors. Better thermal fluids mean better energy capture and lower energy losses, translating into more cost-effective and high-performance systems for consumers and businesses alike.

Lastly, when we look at the environment, this study supports efforts to reduce our dependence on fossil fuels. By boosting the efficiency of solar thermal systems, we can produce more energy with less environmental impact. That means lower carbon emissions, less pollution, and a step forward in protecting our planet for future generations.

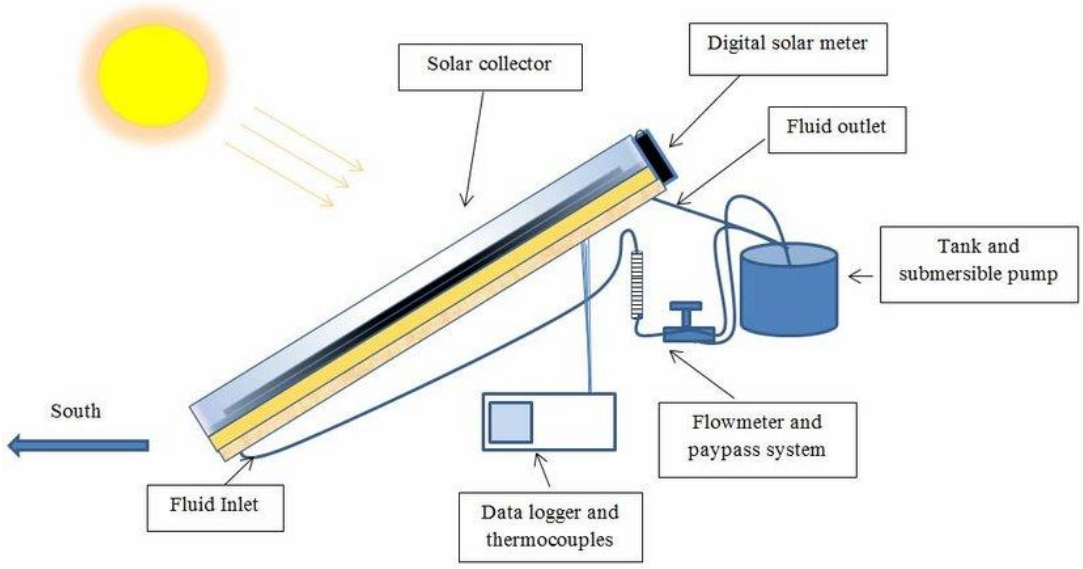

Figure 4: The Schematic of Flat Solar Collector

1.11 Scope and Limitation

This research is limited to two-dimensional, laminar boundary-layer flow of a Powell-Eyring hybrid nanofluid past an infinite flat plate is modelled. The plate may be horizontal or inclined. Using A binary Cu-Al_2O_3/EG-H_2O hybrid nanofluid is treated as a single-phase homogeneous mixture. The momentum-energy system incorporates MHD, thermal radiation, joule heating, Newtonian heating. Boundary-layer and similarity approximations reduce the PDE set to coupled, high-order ODEs. These are solved with a Block Backward Differentiation Formula (BBDF) and MATLAB's bvp5c solver to form a validated numerical result. Outputs include skin-friction coefficient C_xf, local Nusselt number Nu_x,

1.12 Assumption

1.13 Thesis Outline

CHAPTER 2
LITERATURE REVIEW

2.1 Introduction

2.2 Hybrid Nanofluids (HNFs) with Cu and Al_2O_3 with Ethylene Gylcol

Hybrid nanofluids (HNFs) generally have a better thermal conductivity and heat transfer capabilities compared to traditional fluids and mono nanofluids. The idea starts emerging in 2010s, such as Suresh et al. (2012) and Madhesh & Kalaiselvam (2014), in an experimental work to enhance further the heat transfer capability in non-Newtonian fluids, nanofluids, by implementing hybrid between two nanofluids, Alumina (Al_2O_3) and Copper (Cu). The combination of different nanoparticles, such as Cu and Al_2O_3, in a base fluid like water or ethylene glycol, enhances the thermal performance significantly. Cu-Al_2O_3/EG-H_2O.

There is debate on the most effective combinations of nanoparticles for specific applications. Different studies highlight various combinations like Cu-Al_2O_3, Fe_3O_4-MWCNT, and ZnO-Al_2O_3-SiO_2, each showing unique advantages. The debate continues the best nanoparticle volume fractions and their impact on thermal efficiency and friction factors.

It already being shown that SiO_2 nanoparticles in an ethylene glycol-water base fluid improved the thermal efficiency of a compound parabolic collector by 5% to 11.6% (Khaledi et al., 2023). Saleh & Sundar (2021) found that Fe_3O_4-MWCNT (Multi-walled Carbon Nanitubes) hybrid nanofluids demonstrated a 28.46% increase in thermal conductivity and a 39.22% increase in the heat transfer coefficient at a 0.3% volume concentration. The optimal volume fraction for maximum thermal efficiency was 0.3%, balancing thermal conductivity and friction factor.

2.3 Magnetohydrodynamics Effect

The application of magnetic fields in MHD flows of hybrid nanofluids can control and enhance heat transfer rates. Magnetic parameters generally reduce velocity

profiles but increase temperature profiles, contributing to better thermal management. An increased magnetic field parameter generally reduces the velocity profile due to the Lorentz force but increases the temperature profile through enhanced heat transfer. For instance, in a study by Saleh & Sundar (2021) involving a radially stretching sheet, the magnetic field reduced velocity but increased temperature due to the Lorentz force.

By performing research on unsteady inclined magnetohydrodynamic (MHD) Powell-Eyring fluid with microorganisms, Parmar et al. (2024) find out that there is a direct relationship in which the increase in heat generation and nonlinear radiation lead to higher temperature distribution.

Although a study by Bibi et al. (2023) looks at a Newtonian fluid, its findings give valuable insight to compare with Powell-Eyring flows. It shows that when thermal diffusion (Soret effect) and viscous heating (Eckert number) increase, the fluid's velocity and temperature also rise. At the same time, a stronger magnetic field slows the flow, something we also expect in Powell-Eyring models. These results help us understand how MHD and heat-related effects could influence more complex, non-Newtonian flows over a flat plate with thermal radiation.

Adilla Norzawary et al. (2023) shows two nanoparticles give improved heat transfer over single cases, at the cost of higher skin friction. It confirms dual solutions with suction stabilizing the first branch. The study importantly strengthens the numerical approach and provides baseline comparisons that later MHD and radiative studies can build upon.

This also have been researched before by N. A. Khan et al. (2015) where their study on steady Powell-Eyring flow shows that Joule heating (via the Eckert number) and thermal radiation significantly raise the fluid temperature, which is critical in modelling heat transfer in MHD flows. It also confirms that MHD (magnetic field) induces Lorentz forces, which reduce velocity but enhance thermal profiles, behaviours essential for flat plate thermal boundary layers in Powell-Eyring fluid systems. The research by Naseem et al. (2023) also concludes with the same outcomes.

Maiti & Mukhopadhyay (2025) demonstrated that Newtonian heating significantly enhances temperature distribution in Powell-Eyring fluids by strengthening surface-to-fluid heat transfer.

There is a need for more comprehensive models that integrate various physical phenomena such as magnetohydrodynamics, porosity, thermal radiation, and heat generation/absorption in hybrid nanofluid systems for specific application. Current models often lack the ability to predict the behaviour of these complex systems accurately.

2.4 Powell-Eyring Model

Non-Newtonian fluids show distinct rheological behaviour that can be advantageous in thermal conductivity and heat transfer. The Casson model is frequently used to describe the behaviour of non-Newtonian hybrid nanofluids. There is also other more frequently used model like Carreau-Yasuda model and the Reiner-Philippoff model (Alrashdi, 2023; Mohamad et al., 2024). However, it is very few research that use Powell-Eyring model.

In an article by Alrashdi (2023), it is written that he uses Carreau-Yasuda model as her base model on the non-Newtonian rheological properties to study the behaviour of graphene nano-powder and ethylene glycol during peristalsis

Mohamad et al. (2024) uses Reiner-Philippoff model to study Cu-Al_2O_3 and Ag-TiO2 hybrid nanoparticles in nanofluids and find out that it experiences thinning and thickening under shear stress at it molecular states.

Rashad et al. (2023) introduced the Powell–Eyring non-Newtonian model into a hybrid nanofluid context. They investigate mixed convection flow of a Powell-Eyring hybrid nanofluid past a vertical plate embedded in a porous medium, including thermal radiation and internal heat generation. They use Cu-Fe_3O_4 /EG as the hybrid nanofluid. The study is notable for combining magnetic field, thermal radiation, porous media, and a non-Newtonian (Powell-Eyring) hybrid nanofluid. They solved the non-similar boundary-layer equations using a hybrid scheme: local non-similarity with

RKF45 with shooting. The main finding is increasing magnetic field (Hartmann number) implies reduced velocity, drag changes, and overall decrease in heat transfer rate (Nusselt number), and increasing thermal radiation and heat generation cause raised wall temperature and increased Nusselt number (heat transfer). The model has a kinetic-theory basis and reduces to Newtonian behavior at shear extremes, overcoming shortcomings of power-law and Spriggs models

A study by Challa et al. (2025) explores how Powell-Eyring nanofluid behaves as it flows over an unsteady stretching surface under the effects of Stefan blowing or suction. The study shows that as the Brownian motion parameter increases; the fluid's temperature rises while the concentration of nanoparticles decreases. Additionally, an increase in the magnetic number leads to a reduction in the velocity profile.

2.5 Nanoparticle Characteristics

Researchers generally agree that the size, shape, and material of nanoparticles play a significant role in determining the thermal and rheological properties of hybrid nanofluids. Smaller nanoparticles tend to provide better thermal conductivity, while the shape can influence flow behaviour and stability.

Adun et al. (2021) showed that smaller nanoparticles improve thermal conductivity more efficiently. Arguably that their larger surface area allows better heat transfer. Research on the shape of nanoparticle effect the rheology of nanofluids has been conducted by Tabassum & Mehmood (2020) where they found out that surface shear stress increases with the viscosity variation parameter but decreases as the material constant rises. Among the tested types, blade-shaped nanoparticles show the highest effectiveness in enhancing heat transfer in this scenario.

One of the primary challenges in the application of hybrid nanofluids is their stability. Based on the review by Manimaran et al. (2025), nanoparticles tend to agglomerate, which can significantly affect the thermal properties and efficiency of the nanofluids because of van der Waals attraction between particles, arguably by reducing the thermal conductivity and increase the viscosity. One of the solutions for this is as proposed by Mane & Hemadri (2022), where surfactants can greatly enhance the

stability of nanofluids by preventing nanoparticle agglomeration. However, it still requires further research into more methods to enhance the stability of these fluids.

2.6 Temperature Effect

There is an ongoing debate regarding how temperature affects the thermal conductivity of hybrid nanofluids. Some studies suggest that thermal conductivity increases with temperature, while others indicate a more complex relationship that may involve phase changes or other factors. This inconsistency leads to discussions on the need for standardized testing conditions and methodologies.

Shahsavar et al. (2019) had shown how the thermal conductivity of hybrid nanofluids can be temperature-dependent, which influences their heat transfer performance under varying thermal conditions.

2.7 Surface Roughness Effect

The influence of surface roughness on the heat transfer characteristics of hybrid nanofluids is a topic of debate. Some researchers argue that increased surface roughness enhances heat transfer due to increased turbulence, while others suggest that it may lead to higher friction losses, thus negating the benefits. This is especially clear in systems like parabolic trough collectors, where M. S. Khan et al. (2021) in their research, change the shape of the fluid tube to add more surface roughness boosts turbulence and helps improve thermal efficiency. This ongoing discussion highlights the need for more experimental studies to clarify the relationship between surface roughness and heat transfer efficiency. As concluded by Kadivar et al. (2021) in their review, despite notable advances, the structure of turbulent flow remains poorly understood. This is largely because there haven't been enough systematic studies, and the wide variety of surface roughness types adds complexity to how flow behaves near surfaces.

2.8 Non-Linear Radiation

According to M. S. Khan et al. (2021), when nonlinear thermal radiation becomes more significant, it helps boost heat transfer within the fluid, leading to a higher overall temperature. However, the effects of non-linear radiation on hybrid

nanofluid flows are not fully understood and require further investigation. Understanding these effects can lead to better optimization of heat transfer systems in solar collectors and other applications.

2.9 Inclined Surface

The inclination of the plate relative to the gravitational vector modifies the buoyancy forces and pressure distribution in convective flows. For a heated plate in air, gravity induces a buoyant force that drives natural convection along the plate. If the plate is vertical (inclination angle 0 degree from vertical), the buoyancy force acts fully in the direction of the plate, maximizing the aiding convective flow. If the plate is tilted toward horizontal (90 degree from vertical), the component of gravity along the plate is reduced (and at exactly horizontal, buoyancy acts upward perpendicular to the plate, not driving flow along it). Thus, increasing the inclination angle (toward horizontal) generally dampens the buoyant flow along the surface. As the plate becomes less vertical, the driving force for free convection decreases, causing lower fluid velocities along the plate and a thinner momentum boundary layer. At the same time, reduced convective motion means heat builds up more in the fluid near the plate, enhancing the thermal boundary layer.

It is important to note how inclination is defined; many researchers measure the angle α from the vertical. In that convention $\alpha = 0$ is vertical and $\alpha = 90°$ is horizontal; an increase in α reduces buoyancy-induced acceleration along the plate. (Some works use the complementary definition from horizontal, which can invert the described trend if not noted.) Aside from buoyancy, inclination can also affect pressure gradients in forced flows (e.g. an inclined stagnation flow will have a component of dynamic pressure along gravity), and it influences the tendency for flow separation in external flows. In inclined free convection, as α approaches 90°, the flow can transition toward a pure horizontal plate scenario where a stable thermal stratification forms above the plate rather than a strong upslope current.

Hayat et al. (2014) demonstrate this effect, when an inclined stretching sheet's angle is raised from vertical toward horizontal, the flow decelerates and the fluid

temperature rises, because buoyancy forces diminish with inclination. Inclination also matters for stability and dual solutions. Aljabali et al. (2025) also confirm the general trends the as the inclination angle increases, the $\cos(\alpha)$ terms reduce the buoyancy effect, which in turn affects heat transfer depending on whether the flow is assisting or opposing.

Anuar et al. (2021) studies Ag–MgO/water hybrid nanofluid flow on an inclined stretching/shrinking sheet with buoyancy (mixed convection) effects. They explicitly include an inclination angle parameter (α) in the governing equations with buoyancy model through the parameter λ, distinguishing assisting ($\lambda > 0$) and opposing ($\lambda < 0$) flows. The study shows that increasing inclination enhances buoyancy, which increases heat transfer (Nusselt number) and skin friction under certain conditions. They found dual branches (stable first solution, unstable second), consistent with boundary-layer separation dynamics

Overall, plate inclination provides a means to tune the relative influence of buoyant forces, with vertical plates promoting stronger convection currents and horizontal plates relying more on pure conduction unless other forcing is present.

2.10 Numerical Method

Different numerical and computational methods are used to model hybrid nanofluid flows, including the Runge-Kutta method, Runge-Kutta-Fehlberg Method (RKF45), bvp5c solver, Finite Element Method (FEM). The choice of modelling approach can significantly affect the results, leading to debates on the most accurate and reliable methods.

Block Backward Differentiation Formulas (BBDF) are greatly useful for stiff ordinary differential equations (ODE). It is necessary to convert boundary value problem (BVP) into initial value problem (IVP) to implement this method. This paper will implement a stable 4^{th} order BBDF with independent parameter that has been developed by Ibrahim et al. (2019), on the entropy analysis of heat transfer in the hybrid nanofluid.

2.11 Conclusion

From the literature review, it shows that there is limited studies on Powell-Eyring hybrid nanofluids, especially for specific real-world application such as on inclined surface of flat solar collector. The engineering world is in need of comprehensive model which have MHD mixed convection flow of a Powell-Eyring hybrid nanofluid over an inclined plate with thermal radiation to be implemented in the renewable energy applications. By doing so, we can discover interactions that previous isolated studies could not. For example, how non-Newtonian viscosity might alter the optimal nanoparticle fraction or how it influences dual solution behavior in inclined flows.

Furthermore, there is also lack of systematic comparison of numerical methods for these equations. Most of the studies typically uses one numerical method just to solve the equations, but this raise a question that there might be using a counter-productive numerical method for their application. Hence, it is possible that minor discrepancies between papers are due to numerical error or insufficient convergence. It is required for a further study on how to explain the discrepancies from numerical perspective in addition to the physical effects by the fluid itself.

This proposed research will address the current literature gaps by providing a unified, well-vetted analysis of MHD hybrid nanofluid flow on inclined surfaces using the Powell-Eyring model. It will clarify inconsistent results by enforcing consistent definitions and exploring the full parameter space, thereby contributing both to theory (better models and methods) and practice (clear guidelines for use of hybrid nanofluids in MHD convective cooling).

CHAPTER 3
RESEARCH METHODOLOGY

3.1 Introduction

This study's methodology begins by deriving a physics-specific boundary-layer model for a Powell-Eyring hybrid nanofluid, embedding non-Newtonian shear-thinning rheology, dual-nanoparticle mixture rules, viscous dissipation, thermal radiation and magnetic forcing into the momentum-energy equations. To secure numerical credibility, the governing equations after similarity reduction are solved by a global fifth-order Lobatto collocation scheme (MATLAB bvp5c) that supplies adaptive-mesh accuracy and built-in linear-stability eigen-analysis. Once the solvers are mutually validated against Newtonian and single-particle benchmarks, it is swept across a multidimensional parameter space (hybrid nanoparticle volume fraction, shrinking/stretching ratio, suction/blowing strength, curvature and magnetic numbers); from each run the skin-friction coefficient, local Nusselt number, boundary-layer thickness and smallest stability eigenvalue are extracted and mapped, producing design charts that pinpoint operating windows where heat-transfer enhancement is maximised without sacrificing flow stability or incurring excessive drag. Mathematical modelling of non-Newtonian Powell-Eyring hybrid nanofluid.

3.2 Mathematical modelling

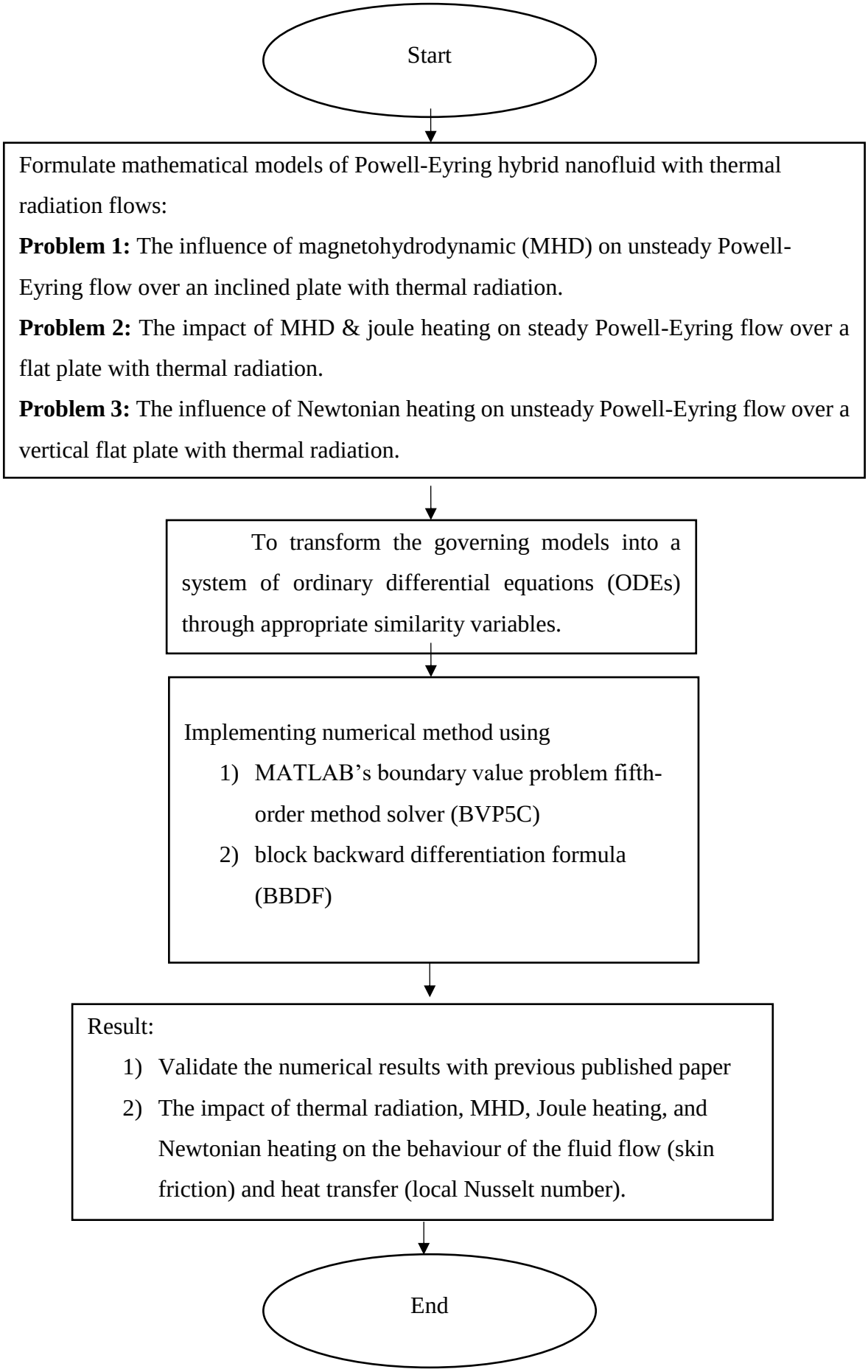
Start
Formulate mathematical models of Powell-Eyring hybrid nanofluid with thermal radiation flows:
Problem 1: The influence of magnetohydrodynamic (MHD) on unsteady Powell-Eyring flow over an inclined plate with thermal radiation.
Problem 2: The impact of MHD & joule heating on steady Powell-Eyring flow over a flat plate with thermal radiation.
Problem 3: The influence of Newtonian heating on unsteady Powell-Eyring flow over a vertical flat plate with thermal radiation.
To transform the governing models into a system of ordinary differential equations (ODEs) through appropriate similarity variables.
Implementing numerical method using
1) MATLAB's boundary value problem fifth-order method solver (BVP5C)
2) block backward differentiation formula (BBDF)
Result:
1) Validate the numerical results with previous published paper
2) The impact of thermal radiation, MHD, Joule heating, and Newtonian heating on the behaviour of the fluid flow (skin friction) and heat transfer (local Nusselt number).
End

3.2.1 Governing equations

Considering an incompressible, single-phase advection-diffusion model for a hybrid nanofluid with constant effective properties density of HNFs ρ_{hnf}, dynamic viscosity of the HNFs μ_{hnf}, thermal conductivity of the HNFs k_{hnf}, and volumetric heat capacity $\left(\rho C_p\right)_{hnf}$. The concerned governing equations for these problems can be written as:

$$\nabla \cdot V = 0 \tag{1.1}$$

$$\frac{\partial V}{\partial t} + \left(V \bullet \nabla\right)V = -\frac{1}{\rho_{hnf}}\nabla \mathrm{p} + \frac{\mu_{hnf}}{\rho_{hnf}}\nabla^2 V \tag{1.2}$$

$$\frac{\partial T}{\partial t} + \left(V \bullet \nabla\right)T = -\frac{k_{hnf}}{\left(\rho C_p\right)_{hnf}}\nabla^2 T \tag{1.3}$$

Where (1.1) is continuity equation, (1.2) is momentum equation, and (1.3) is energy equation. This PDEs instantiate the continuum balance laws closed by a rheology and mixture correlations for hybrid effective properties. This governing model stands on the consideration of continuum mechanics and Fourier-Newton transport (combination of conduction inside a fluid with convection at its boundary).

By using the boundary layer approximation, equations (1) - (3) with Powell-Eyring model can be reduced to boundary layer equations in the form of PDEs as follows,

$$\frac{\partial u}{\partial x} + \frac{\partial v}{\partial y} = 0 \tag{1.4}$$

$$\frac{\partial u}{\partial t} + u\frac{\partial u}{\partial x} + v\frac{\partial v}{\partial y} = \left(\nu_{hnf} + \frac{1}{\rho_{hnf}\beta\varsigma}\right)\frac{\partial^2 u}{\partial y^2} - \frac{1}{2\beta\varsigma^3\rho_{hnf}}\left(\frac{\partial u}{\partial y}\right)^2\frac{\partial^2 u}{\partial y^2} \tag{1.5}$$

$$\frac{\partial T}{\partial t} + u\frac{\partial T}{\partial x} + v\frac{\partial T}{\partial y} = \frac{k_{\mathrm{hnf}}}{(\rho C_p)_{\mathrm{hnf}}}\left[\frac{\partial^2 T}{\partial y^2}\right] - \frac{1}{(\rho C_p)_{\mathrm{hnf}}}\left[\frac{\partial q_r}{\partial y}\right] + \frac{\mu_{\mathrm{hnf}}}{(\rho C_p)_{\mathrm{hnf}}}\left[\frac{\partial u}{\partial y}\right]^2 \tag{1.6}$$

$$u = U_w + \mu_{\mathrm{hnf}}\left[\frac{\partial u}{\partial y}\right], \quad v = V_w, -k_f\left[\frac{\partial T}{\partial y}\right] = h_f\left(T_w - T\right), y = 0 \tag{1.7}$$

$$u \to 0, \quad T \to T_\infty \quad \text{as } y \to \infty \tag{1.8}$$

Where (1.4) is continuity equation, (1.5) is momentum equation, (1.6) is energy equation, (1.7) and (1.8) is the boundary condition (Aziz et al., 2021). This is unsteady, 2-D boundary-layer balance laws for a hybrid nanofluid with extra stress considerations using Powell-Eyring non-Newtonian constitutive model. The momentum equation (1.5) consist of convection with Powell-Eyring diffusion/retardation terms using an effective kinematic viscosity v_{hnf} for hybrid-nanofluid properties. The energy equation (1.6) consist of convection and conduction with thermal conductivity of the HNFs k_{hnf}, radiative heat flux gradient $\frac{\partial q_r}{\partial y}$, and viscous dissipation $\frac{\mu_{\text{hnf}}}{(\rho C_p)_{\text{hnf}}}\left[\frac{\partial u}{\partial y}\right]^2$. The boundary condition (1.7) and (1.8) represent Navier slip at the wall u, suction/blowing v, and convective wall heating $h_f(T_w - T)$.

3.2.2 Applying similarity transformation

To obtain the ordinary differential equation (ODEs) from the model, similarity variables need to be implemented, which are given as,

$$\begin{aligned}
&u = \frac{\partial \psi}{\partial y}, \quad v = -\frac{\partial \psi}{\partial x}, \\
&\eta(x, y) = \sqrt{\frac{c}{\nu_f (1 - \varpi t)}}\, y, \\
&\psi(x, y) = \sqrt{\frac{\nu_f c}{1 - \varpi t}}\, x f(\eta), \\
&\theta(\eta) = \frac{T - T_\infty}{T_w - T_\infty}
\end{aligned} \tag{1.9}$$

Where u and v are redefined in a stream function form ψ, x and y redefined in term of similarity variable η with the stream function ψ, and the thermal function for the ratio of the difference in the temperature T in the fluid and temperature at wall T_w with ambient temperature T_∞. This similarity equations are necessary to converts a messy, coupled, time-dependent 2-D Newtonian boundary layer system into a

boundary-value problem in η. This is to enables robust BVP solvers like BVP5C with provable error control.

3.3 Numerical computation

The reduced ODEs (8) - (9) will be solved numerically using a boundary value problem-solver available in MATLAB software. The solver known as bvp5c is the embedded formula of the 3-stage Lobatto IIIa (Runge-Kutta family), an efficient numerical method for solving one or two unknown boundary value problems. The computational flow is given as follows:

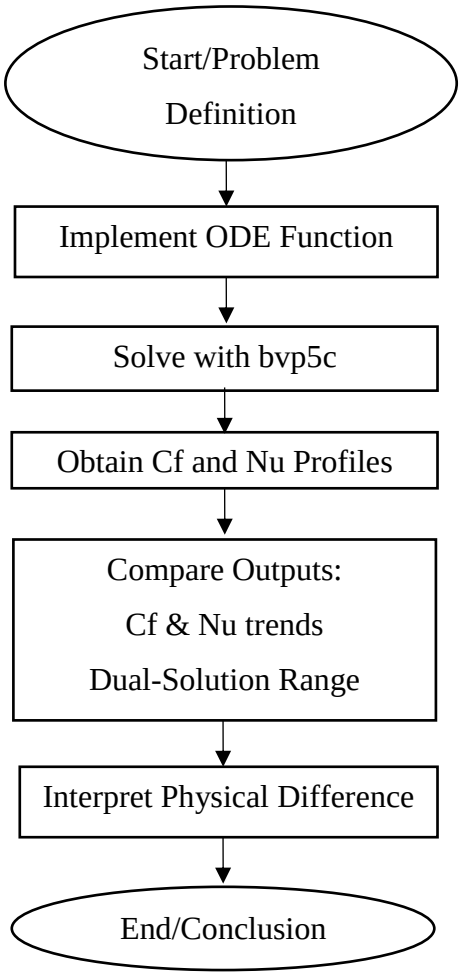
Start/Problem
Definition
Implement ODE Function
Solve with bvp5c
Obtain Cf and Nu Profiles
Compare Outputs:
Cf & Nu trends
Dual-Solution Range
Interpret Physical Difference
End/Conclusion

3.4 Thermophysical Properties and Characteristics

Table 1: Formula of thermophysical properties for hybrid nanofluid (Takabi & Salehi, 2014; Zainal et al., 2021)

Thermophysical Properties	Hybrid Nanofluid Formula
Density	$\rho_{hnf} = (1-\phi_{hnf})\rho_f + \phi_1\rho_{s1} + \phi_2\rho_{s2}$
Dynamic Viscosity	$\frac{\mu_{hnf}}{\mu_f} = \frac{1}{(1-\phi_{hnf})^{2.5}}$
Heat Capacity	$(\rho c_p)_{hnf} = (1-\phi_{hnf})(\rho c_p)_f + \phi_1(\rho c_p)_{s1} + \phi_2(\rho c_p)_{s2}$
Electrical Conductivity	$\frac{\sigma_{hnf}}{\sigma_f} = \frac{\left(\frac{\phi_1\sigma_{s1}+\phi_2\sigma_{s2}}{\phi_{hnf}} + 2\sigma_f + 2(\phi_1\sigma_{s1}+\phi_2\sigma_{s2}) - 2\phi_{hnf}\sigma_f\right)}{\left(\frac{\phi_1\sigma_{s1}+\phi_2\sigma_{s2}}{\phi_{hnf}} + 2\sigma_f - (\phi_1\sigma_{s1}+\phi_2\sigma_{s2}) + \phi_{hnf}\sigma_f\right)}$
Thermal Conductivity	$\frac{k_{hnf}}{k_f} = \frac{\left(\frac{\phi_1 k_{s1}+\phi_2 k_{s2}}{\phi_{hnf}} + 2k_f + 2(\phi_1 k_{s1}+\phi_2 k_{s2}) - 2\phi_{hnf}k_f\right)}{\left(\frac{\phi_1 k_{s1}+\phi_2 k_{s2}}{\phi_{hnf}} + 2k_f - (\phi_1 k_{s1}+\phi_2 k_{s2}) + \phi_{hnf}k_f\right)}$
Thermal Expansion	$\beta_{hnf} = \frac{1}{\rho_{hnf}}\left[\phi_1\rho_1\beta_1 + \phi_2\rho_2\beta_2 + (1-\phi)\rho_f\beta_f\right]$

Table 2: Formula of thermophysical characteristics for hybrid nanofluid (Aziz et al., 2021)

Thermophysical Char.	ρ (kg/m)	c_p (J/kg·K)	k (W/m·K)	σ (S/m)
Ethylene glycol (EG)	1114	2415	0.252	5.5×10^{-6}
Pure water (H_2O)	997.1	4179	0.613	0.05
Copper (Cu)	8933	385.0	401.00	5.96×10^{7}
Ferro (Fe_3O_4)	5180	670	9.7	0.74×10^{6}
Copper oxide (CuO)	6510	540	18	5.96×10^{7}
Alumina (Al_2O_3)	3970	765.0	40.000	3.5×10^{7}
Titanium oxide (TiO_2)	4250	686.2	8.9538	2.38×10^{6}

3.5 Evaluation of the computed data

CHAPTER 4
THE INFLUENCE OF MAGNETOHYDRODYNAMIC (MHD) ON UNSTEADY POWELL-EYRING FLOW OVER AN INCLINED PLATE ON POWELL-EYRING HYBRID NANOFLUID WITH THERMAL RADIATION FLOW

4.1 Introduction

Many practical flows involve inclined surfaces (such as tilted solar collectors or inclined heat exchangers) where gravity influences the boundary layer differently than on horizontal or vertical plates. Adding a magnetic field (MHD) enables flow control and is pertinent to cooling of electronic devices and MHD generators, though it tends to slow the fluid via Lorentz forces. Accounting for thermal radiation in such flows is also crucial at high temperatures, since radiative heat transfer (like an "invisible sunlight" within the fluid) can substantially alter thermal profiles. Finally, conventional Newtonian models may fail to capture the complex rheology of nanofluids at higher particle loadings; hence non-Newtonian frameworks like the Powell-Eyring model are being adopted to more realistically describe viscosity variations. This first problem covers the MHD flow over inclined surfaces with thermal radiation using hybrid nanofluids, highlighting the Powell-Eyring non-Newtonian perspective.

The study investigates a two-dimensional, laminar, incompressible Powell-Eyring hybrid nanofluid flow over a flat plate, which may be oriented horizontally or at an incline. The working fluid is a binary hybrid nanofluid composed of Cu-Al_2O_3 nanoparticles uniformly dispersed in an ethylene glycol–water base, modelled as a single-phase continuum. The physical formulation accounts for magnetohydrodynamic (MHD) effects through a transverse magnetic field. A nonlinear thermal radiation modelled using the Rosseland diffusion approximation. Key assumptions include laminar two-dimensional flow, uniform nanoparticle dispersion, the significance of viscous dissipation, and the neglect of induced magnetic fields under the low magnetic Reynolds number condition. The boundary layer equations for this problem are:

Continuity Equation: $\frac{\partial u}{\partial x}+\frac{\partial v}{\partial y}=0$ (1.10)

$$\frac{\partial u}{\partial t}+u\frac{\partial u}{\partial x}+v\frac{\partial u}{\partial y}=\left(\nu_{hnf}+\frac{1}{\rho_{hnf}\beta\varsigma}\right)\frac{\partial^2 u}{\partial y^2}$$

Momentum Equation: $-\frac{1}{2\beta\varsigma^3\rho_{hnf}}\left(\frac{\partial u}{\partial y}\right)^2\frac{\partial^2 u}{\partial y^2}$ (1.11)

$$-\frac{\sigma_{\text{hnf}}B^2}{\rho_{\text{hnf}}}u+g\beta_{hnf}(T-T_\infty)\cos\alpha$$

$$\frac{\partial T}{\partial t}+u\frac{\partial T}{\partial x}+v\frac{\partial T}{\partial y}=\frac{k_{\text{hnf}}}{(\rho C_p)_{\text{hnf}}}\left[\frac{\partial^2 T}{\partial y^2}\right]$$

Energy Equation: $-\frac{1}{(\rho C_p)_{\text{hnf}}}\left[\frac{\partial q_r}{\partial y}\right]$ (1.12)

$$+\frac{\mu_{\text{hnf}}}{(\rho C_p)_{\text{hnf}}}\left[\frac{\partial u}{\partial y}\right]^2$$

Subject to boundary conditions:

$$u(x,y)=U_w+L\left[\frac{\partial u}{\partial y}\right], v(x,y)=V_w, -k_f\left[\frac{\partial T}{\partial y}\right]=h_f(T_w-T) \text{ where } y=0 \quad (1.13)$$

$$u\to 0,\quad T\to T_\infty \text{ as } y\to\infty \qquad (1.14)$$

Pr	Ishak	Nazar	Das	Aziz	Abolbashari	Present
0.72	0.8086	0.8086	0.80876122	0.80876181	0.80863135	0.808631352
1.0	1.0000	1.0000	1.00000000	1.00000000	1.00000000	1.000000000
3.0	1.9237	1.9236	1.92357431	1.92357420	1.92368259	1.923682569
7.0	3.0723	3.0722	3.07314679	3.07314651	3.07225021	3.072250190
10	3.7207	3.7006	3.72055436	3.72055429	3.72067390	3.720673885

Table 3: Comparison of $\theta'(0)$ with variation of Prandtl number (Aziz et al., 2021)

A	Chempaka	Kumar &	Pal	Present

	et. al.	Srinivas		
0.8	-1.26151	-1.26108	-1.26104	-1.26104
1.2	-1.37805	-1.37777	-1.37772	-1.37772

Table 4: Comparison of $f''(0)$ with variation of A when Pr=0 (Kumar & Srinivas, 2020)

M	Prasad et. al.	Mukhopadhyay et. al.	Palani et. al.	Olkha et. al.	Present
0.0	1.0001743	1.0001731	1.000000	1.000008389	1.000000000
0.5	1.2247532	1.2247531	1.2247452	1.224744917	1.224744871
1	1.4144491	1.4144503	1.4142141	1.414213563	1.414213562
1.5	1.5811391	1.5811402	1.5811394	1.581138831	1.581138830
2	1.7322032	1.7322033	1.7320512	1.732050806	1.732050808

Table 5: Comparison of $-f''(0)$ with variation of M when Pr=0.72 (Olkha & Dadheech, 2021)

α	Krishna et al.	Present
0	0.487717	0.083678578
$\frac{\pi}{4}$	0.635062	0.416070068
$\frac{\pi}{3}$	0.743444	0.675465398

Table 6: Comparison of $-f''(0)$ with variation of α when $\lambda = 1$ and S=1 (Krishna et al., 2016)

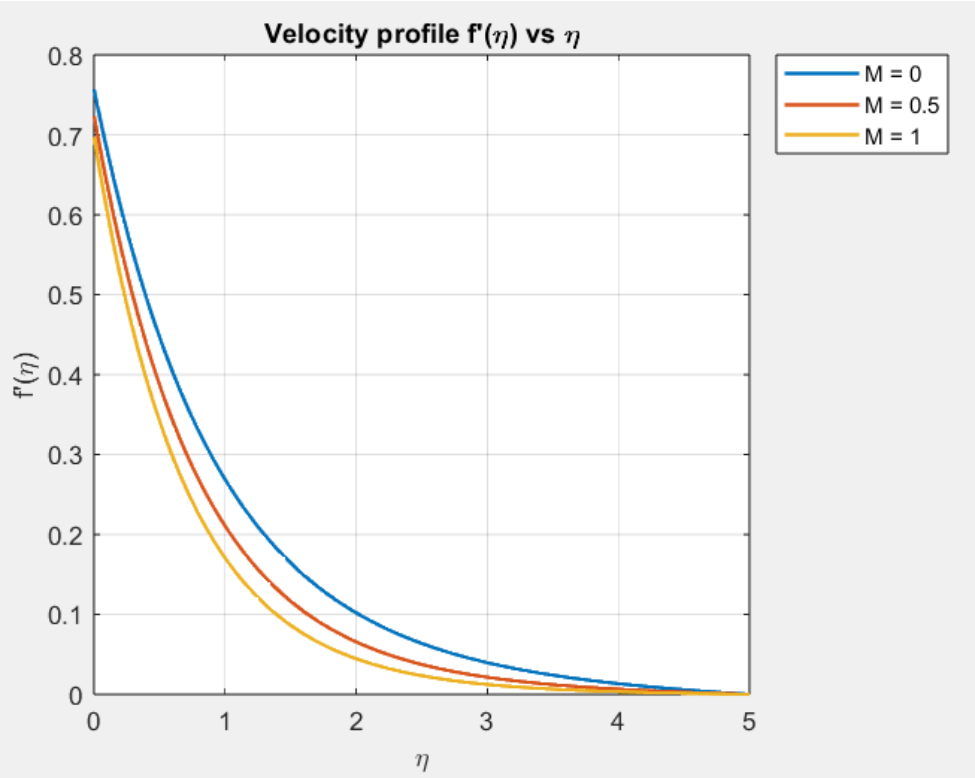
Velocity profile f'(η) vs η
M = 0
M = 0.5
M = 1
f'(η)
η
0
0.1
0.2
0.3
0.4
0.5
0.6
0.7
0.8
0
1
2
3
4
5

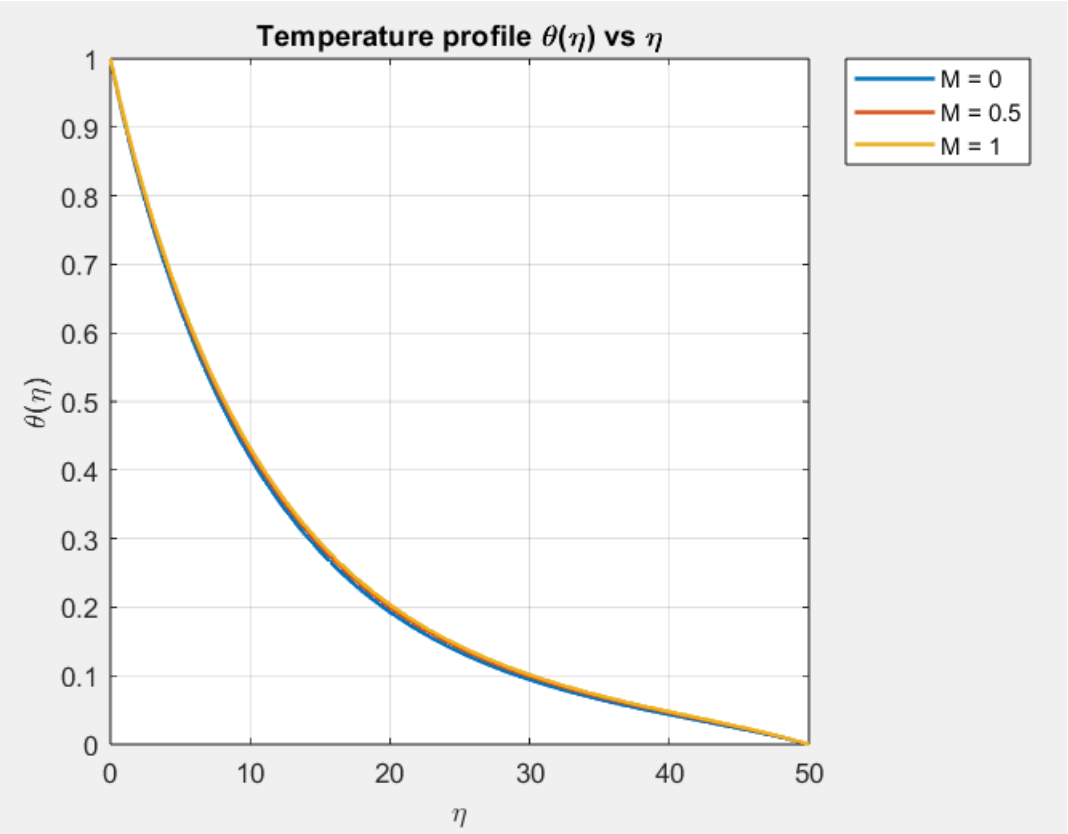


```
delta=0.2;
omega=0.1;
A=0.2;
M=0.01; % our value
lambda=0.2; % our value
Pr=6.2;
Rd=0.2;
Ec=0.2;
S=0.1;
Sl=0.3; % slip parameter
Bi=0.2;
alpha=pi/2; % our value

% Al2O3-Cu/H2O
phi1=0.09; phi2=0.09; phiHnf=phi1+phi2;
rhoS1=3970; rhoS2=8933; rhoF=997.1;
betaS1=(0.85*(10^-5)); betaS2=(1.67*(10^-5)); betaF=21;
```

sigmaS1=(3.5*(10^7)); sigmaS2=(5.96*(10^7)); sigmaF=0.05;
CpS1=765; CpS2=385; CpF=4179;
kS1=40; kS2=401; kF=0.613;

// Need to also add the formula equation for proporsal

CHAPTER 5
CONCLUSION

5.1 Introduction

REFERENCES

Adilla Norzawary, N. H., Soid, S. K., Ishak, A., Anuar Mohamed, M. K., Khan, U., Sherif, E. S. M., & Pop, I. (2023). Stability analysis for heat transfer flow in micropolar hybrid nanofluids. *Nanoscale Advances*, *5*(20), 5627–5640. https://doi.org/10.1039/d3na00675a

Adun, H., Wole-Osho, I., Okonkwo, E. C., Kavaz, D., & Dagbasi, M. (2021). A critical review of specific heat capacity of hybrid nanofluids for thermal energy applications. *Journal of Molecular Liquids*, *340*. https://doi.org/10.1016/j.molliq.2021.116890

Aljabali, A., Kasim, A. R. M., Waini, I., Khashi'ie, N. S., & Tijani, Y. O. (2025). Thermal Analysis of Eyring-Powell Hybrid Nanofluid: A Case of Combined Convective Transport and Radiative Heat Flux along Inclined Stretching/Shrinking Sheet. *WSEAS Transactions on Heat and Mass Transfer*, *20*, 1–13. https://doi.org/10.37394/232012.2025.20.1

Alrashdi, A. M. A. (2023). Mixed convection and thermal radiation effects on non-Newtonian nanofluid flow with peristalsis and Ohmic heating. *Frontiers in Materials*, *10*. https://doi.org/10.3389/fmats.2023.1178518

Aminuddin, N. A. (2024). *Effects of non-newtonian hybrid nanofluid heat transfer and entropy generation over a horizontal shrinking surface* [Master Thesis]. Universiti Pertahanan Nasional Malaysia.

Anuar, N. S., Bachok, N., & Pop, I. (2021). Influence of buoyancy force on Ag-MgO/water hybrid nanofluid flow in an inclined permeable stretching/shrinking sheet. *International Communications in Heat and Mass Transfer*, *123*. https://doi.org/10.1016/j.icheatmasstransfer.2021.105236

Asshaari, I., & Md Jedi, M. A. (2022). *Nanobendalir Mono dan Hibrid Pendekatan Statistik dalam Mekanik Bendalir* (1st ed.). Penerbit Universiti Kebangsaan Malaysia.

Aziz, A., Jamshed, W., Aziz, T., Bahaidarah, H. M. S., & Ur Rehman, K. (2021). Entropy analysis of Powell–Eyring hybrid nanofluid including effect of linear thermal radiation and viscous dissipation. *Journal of Thermal Analysis and Calorimetry*, *143*(2), 1331–1343. https://doi.org/10.1007/s10973-020-10210-2

Bibi, S. K. N., Padma, G., & Sailaja, P. (2023). Soret effect on an unsteady MHD free convective flow past an infinite vertical plate with constant suction. *Materials*

Today: Proceedings, *92*, 1518–1525. https://doi.org/10.1016/j.matpr.2023.05.723

Challa, K. K., Rao, M. E., Jawad, M., Saidani, T., Ali Osman Abdallah, S., & D, T. (2025). Enhanced heat transfer and flow dynamics of Powell-Eyring nanofluid: unsteady stretched surface and with Stefan blowing/suction. *Case Studies in Thermal Engineering*, *65*. https://doi.org/10.1016/j.csite.2024.105664

Escudier, M., & Atkins, T. (2019). *A Dictionary of Mechanical Engineering*. Oxford University Press. https://doi.org/10.1093/acref/9780198832102.001.0001

Hayat, T., Asad, S., Mustafa, M., & Alsaedi, A. (2014). Radiation effects on the flow of powell-eyring fluid past an unsteady inclined stretching sheet with non-uniform heat source/sink. *PLoS ONE*, *9*(7). https://doi.org/10.1371/journal.pone.0103214

Ibrahim, Z. B., Shah, I., & Zawawi, M. (2019). A Stable Fourth Order Block Backward Differentiation Formulas (α) for Solving Stiff Initial Value Problems. In *ASM Sci. J., Special Issue* (Vol. 6).

Jusoh, R., Ismail, Z., Mohamed, M. K. A., & Zainuddin, N. (2024). Magnetohydrodynamics Cu-TiO2 Hybrid Nanofluid with Viscous Dissipation. In S. Shafie & L. Y. Jiann (Eds.), *Hybrid Nanofluids and Its Model Applications* (1st ed., pp. 35–62). Penerbit UTM Press.

Kadivar, M., Tormey, D., & McGranaghan, G. (2021). A review on turbulent flow over rough surfaces: Fundamentals and theories. In *International Journal of Thermofluids* (Vol. 10). Elsevier B.V. https://doi.org/10.1016/j.ijft.2021.100077

Khaledi, O., Saedodin, S., & Rostamian, S. H. (2023). Experimental investigation of thermal efficiency and thermal performance improvement of compound parabolic collector utilizing SiO2/Ethylene glycol–water nanofluid. *Environmental Science and Pollution Research*, *30*(5), 12169–12188. https://doi.org/10.1007/s11356-022-22848-6

Khan, M. S., Abid, M., Yan, M., Ratlamwala, T. A. H., & Mubeen, I. (2021). Thermal and thermodynamic comparison of smooth and convergent-divergent parabolic trough absorber tubes with the application of mono and hybrid nanofluids. *International Journal of Energy Research*, *45*(3), 4543–4564. https://doi.org/10.1002/er.6123

Khan, N. A., Sultan, F., & Khan, N. A. (2015). Heat and mass transfer of thermophoretic MHD flow of powell-eyring fluid over a vertical stretching sheet in the presence of chemical reaction and joule heating. *International Journal of*

Chemical Reactor Engineering, *13*(1), 37–49. https://doi.org/10.1515/ijcre-2014-0090

Krishna, P. M., Sandeep, N., Reddy, J. V. R., & Sugunamma, V. (2016). Dual solutions for unsteady flow of Powell-Eyring fluid past an inclined stretching sheet. *Journal of Naval Architecture and Marine Engineering*, *13*(1), 89–99. https://doi.org/10.3329/jname.v13i1.25338

Kumar, B., & Srinivas, S. (2020). Unsteady hydromagnetic flow of eyring-powell nanofluid over an inclined permeable stretching sheet with Joule Heating and thermal radiation. *Journal of Applied and Computational Mechanics*, *6*(2), 259–270. https://doi.org/10.22055/JACM.2019.29520.1608

Law, J., & Rennie, R. (2020). *A Dictionary of Chemistry*. Oxford University Press. https://doi.org/10.1093/acref/9780198841227.001.0001

Madhesh, D., & Kalaiselvam, S. (2014). Experimental analysis of hybrid nanofluid as a coolant. *Procedia Engineering*, *97*, 1667–1675. https://doi.org/10.1016/j.proeng.2014.12.317

Maiti, H., & Mukhopadhyay, S. (2025). Insight into Eyring–Powell nanofluid flow over a radially stretching disk with Stefan blowing, nonlinear thermal radiation and Newtonian heating. *Multiscale and Multidisciplinary Modeling, Experiments and Design*, *8*(6). https://doi.org/10.1007/s41939-025-00860-w

Mane, N. S., & Hemadri, V. (2022). Experimental Investigation of Stability, Properties and Thermo-rheological Behaviour of Water-Based Hybrid CuO and Fe3O4 Nanofluids. *International Journal of Thermophysics*, *43*(1). https://doi.org/10.1007/s10765-021-02938-2

Manimaran, M., Norizan, M. N., Kassim, M. H. M., Adam, M. R., Abdullah, N., & Norrrahim, M. N. F. (2025). Critical review on the stability and thermal conductivity of water-based hybrid nanofluids for heat transfer applications. In *RSC Advances* (Vol. 15, Issue 18, pp. 14088–14125). Royal Society of Chemistry. https://doi.org/10.1039/d5ra00844a

Mohamad, N., Khan, U., & Ishak, A. (2024). Assessing the Efficacy of Hybrid Nanofluid within a Non-Newtonian Reiner-Philippoff Model, Incorporating MHD and Thermal Radiation Past a Stretching/Shrinking Sheet. *PaperASIA*, *40*(4b), 165–177. https://doi.org/10.59953/paperasia.v40i4b.199

Naseem, T., Bibi, I., Shahzad, A., & Munir, M. (2023). Analysis of Heat Transport in a Powell-Eyring Fluid with Radiation and Joule Heating Effects via a Similarity

Transformation. *Fluid Dynamics and Materials Processing*, *19*(3), 663–677. https://doi.org/10.32604/fdmp.2022.021136

Olkha, A., & Dadheech, A. (2021). Unsteady magnetohydrodynamics slip flow of powell-eyring fluid with microorganisms over an inclined permeable stretching sheet. *Journal of Nanofluids*, *10*(1), 128–145. https://doi.org/10.1166/JON.2021.1774

Parmar, A., Kumar, P., Choudhary, R., Garg, S., & Jain, A. (2024). Unsteady Inclined MHD Powell-Eyring Fluid with Microorganisms Over an Inclined Permeable Stretching Sheet with Zero Mass Flux and Slip Condition. *International Journal of Applied and Computational Mathematics*, *10*(5). https://doi.org/10.1007/s40819-024-01780-y

Rashad, A. M., Nafe, M. A., & Eisa, D. A. (2023). Heat Generation and Thermal Radiation Impacts on Flow of Magnetic Eyring–Powell Hybrid Nanofluid in a Porous Medium. *Arabian Journal for Science and Engineering*, *48*(1), 939–952. https://doi.org/10.1007/s13369-022-07210-9

Rennie, R., & Law, J. (2019). *A Dictionary of Physics*. Oxford University Press. https://doi.org/10.1093/acref/9780198821472.001.0001

Saleh, B., & Sundar, L. S. (2021). Thermal efficiency, heat transfer, and friction factor analyses of mwcnt + fe3o4/water hybrid nanofluids in a solar flat plate collector under thermosyphon condition. *Processes*, *9*(1), 1–19. https://doi.org/10.3390/pr9010180

Shahsavar, A., Godini, A., Sardari, P. T., Toghraie, D., & Salehipour, H. (2019). Impact of variable fluid properties on forced convection of Fe3O4/CNT/water hybrid nanofluid in a double-pipe mini-channel heat exchanger. *Journal of Thermal Analysis and Calorimetry*, *137*(3), 1031–1043. https://doi.org/10.1007/s10973-018-07997-6

Suresh, S., Venkitaraj, K. P., Selvakumar, P., & Chandrasekar, M. (2012). Effect of Al 2O 3-Cu/water hybrid nanofluid in heat transfer. *Experimental Thermal and Fluid Science*, *38*, 54–60. https://doi.org/10.1016/j.expthermflusci.2011.11.007

Tabassum, R., & Mehmood, R. (2020). Crosswise Transport Mechanism of Micro-rotating Hybrid (Cu–Al2O3/H2O) Nanofluids Through Infusion of Various Shapes of Nanoparticles. *Arabian Journal for Science and Engineering*, *45*(7), 5883–5893. https://doi.org/10.1007/s13369-020-04580-w

Takabi, B., & Salehi, S. (2014). Augmentation of the heat transfer performance of a

sinusoidal corrugated enclosure by employing hybrid nanofluid. *Advances in Mechanical Engineering*, *2014*. https://doi.org/10.1155/2014/147059

The Concise Oxford Dictionary of Mathematics. (2021). Oxford University Press. https://doi.org/10.1093/acref/9780198845355.001.0001

Zainal, N. A., Nazar, R., Naganthran, K., & Pop, I. (2021). Unsteady MHD stagnation point flow induced by exponentially permeable stretching/shrinking sheet of hybrid nanofluid. *Engineering Science and Technology, an International Journal*, *24*(5), 1201–1210. https://doi.org/10.1016/j.jestch.2021.01.018

Zainal, N. A., Nazar, R., Pop, I., & Naganthran, K. (2024). Unsteady Separated Hybrid Stagnation Nanofluid Flow. In S. Shafie & L. Y. Jiann (Eds.), *Hybrid Nanofluids and Its Model Applications* (1st ed., pp. 63–78). Penerbit UTM Press.

Zaman, H., Shah, M. A., & Ibrahim, M. (2013). Unsteady Incompressible Couette Flow Problem for the Eyring-Powell Model with Porous Walls. *American Journal of Computational Mathematics*, *03*(04), 313–325. https://doi.org/10.4236/ajcm.2013.34041

APPENDICES

APPENDIX 1

Formulation for the General Equation For
Problem 1: Powell-Eyring hybrid nanofluid with thermal radiation flow with magnetohydrodynamic (MHD) on unsteady Powell-Eyring flow over an inclined plate with thermal radiation.

Governing equations:

$$\nabla \cdot V = 0 \qquad (1.15)$$

$$\frac{\partial V}{\partial t} + (V \bullet \nabla)V = -\frac{1}{\rho_{hnf}}\nabla \mathrm{p} + \frac{\mu_{hnf}}{\rho_{hnf}}\nabla^2 V \qquad (1.16)$$

$$\frac{\partial T}{\partial t} + (V \bullet \nabla)T = -\frac{k_{hnf}}{(\rho C_p)_{hnf}}\nabla^2 T \qquad (1.17)$$

where (1.15) is continuity equation, (1.16) is momentum equation, and (1.17) is energy equation.

The boundary layer equations in the form of PDE for the 1st problem is given as:

Continuity Equation: $\frac{\partial u}{\partial x} + \frac{\partial v}{\partial y} = 0$ (1.18)

Momentum Equation:

$$\frac{\partial u}{\partial t} + u\frac{\partial u}{\partial x} + v\frac{\partial u}{\partial y} = \left(\nu_{hnf} + \frac{1}{\rho_{hnf}\beta\varsigma}\right)\frac{\partial^2 u}{\partial y^2} - \frac{1}{2\beta\varsigma^3\rho_{hnf}}\left(\frac{\partial u}{\partial y}\right)^2\frac{\partial^2 u}{\partial y^2} - \frac{\sigma_{\mathrm{hnf}}B^2}{\rho_{\mathrm{hnf}}}u + g\beta_{hnf}(T - T_\infty)\cos\alpha \qquad (1.19)$$

Energy Equation:

$$\frac{\partial T}{\partial t} + u\frac{\partial T}{\partial x} + v\frac{\partial T}{\partial y} = \frac{k_{\mathrm{hnf}}}{(\rho C_p)_{\mathrm{hnf}}}\left[\frac{\partial^2 T}{\partial y^2}\right] - \frac{1}{(\rho C_p)_{\mathrm{hnf}}}\left[\frac{\partial q_r}{\partial y}\right] + \frac{\mu_{\mathrm{hnf}}}{(\rho C_p)_{\mathrm{hnf}}}\left[\frac{\partial u}{\partial y}\right]^2 \qquad (1.20)$$

where B is magnetic field, $B = B_0\left(\frac{1}{1-\varpi t}\right)^{\frac{1}{2}}$

Subject to boundary conditions:

$$u(x,y)=U_w+L\left[\frac{\partial u}{\partial y}\right], v(x,y)=V_w, -k_f\left[\frac{\partial T}{\partial y}\right]=h_f(T_w-T) \text{ where } y=0 \quad (1.21)$$

$$u \to 0, \quad T \to T_\infty \text{ as } y \to \infty \qquad (1.22)$$

Where slip parameter,

$$U_w(x,t)=\frac{xc}{1-\varpi t}, T_w(x,t)=T_\infty+\frac{xc}{(1-\varpi t)^2}, \quad L=L_0(1-\varpi t)^{\frac{1}{2}}, h_f=h_{f0}(1-\varpi t)^{-\frac{1}{2}} \qquad (1.23)$$

In order to transform PDE (1.18)-(1.22) into ODE, the similarity variables η with stream function ψ and dimensionless temperature θ are introduced:

$$\eta(x,y)=\sqrt{\frac{c}{\nu_f(1-\varpi t)}}y, \psi(x,y)=\sqrt{\frac{\nu_f c}{1-\varpi t}}xf(\eta) \qquad (1.24)$$

$$\theta(\eta)=\frac{T-T_\infty}{T_w-T_\infty} \qquad (1.25)$$

$$u=\frac{\partial \psi}{\partial y}, \quad v=-\frac{\partial \psi}{\partial x} \qquad (1.26)$$

Where f is a dimensionless stream function, ν_f is -..

Finding u from (1.26):

$$u=\left(\frac{\partial \psi}{\partial \eta}\right)\left(\frac{\partial \eta}{\partial y}\right)$$
$$=\frac{\partial}{\partial \eta}\left(\left(\frac{\nu_f c}{1-\varpi t}\right)^{\frac{1}{2}}xf\right)\frac{\partial}{\partial y}\left(\left(\frac{c}{\nu_f(1-\varpi t)}\right)^{\frac{1}{2}}y\right) \qquad (1.27)$$
$$=\left(\frac{\nu_f c}{1-\varpi t}\right)^{\frac{1}{2}}xf'\left(\frac{c}{\nu_f(1-\varpi t)}\right)^{\frac{1}{2}}$$
$$=\frac{c}{1-\varpi t}xf'$$

Where ` is a differentiation with respect to η .

Finding v from (1.26):

$$v = -\frac{\partial \psi}{\partial x}$$
$$= -\frac{\partial}{\partial x}\left(\left(\frac{\nu_f c}{1-\varpi t}\right)^{\frac{1}{2}} xf\right) \qquad (1.28)$$
$$= -\left(\frac{\nu_f c}{1-\varpi t}\right)^{\frac{1}{2}} f$$

To solve continuity equation (1.18), find du/dx and dv/dy from (1.27) and (1.28) respectively,

$$\frac{\partial u}{\partial x} = \frac{\partial}{\partial x}\left(\frac{c}{1-\varpi t} xf'\right) = \frac{c}{1-\varpi t} f' \quad (1.29)$$

$$\frac{\partial v}{\partial y} = \frac{\partial}{\partial y}\left(-\left(\frac{\nu_f c}{1-\varpi t}\right)^{\frac{1}{2}} f\right)$$
$$= -\left(\frac{\nu_f c}{1-\varpi t}\right)^{\frac{1}{2}} \frac{\partial f}{\partial \eta}\frac{\partial \eta}{\partial y} \qquad (1.30)$$
$$= -\left(\frac{\nu_f c}{1-\varpi t}\right)^{\frac{1}{2}} f'\left(\frac{c}{\nu_f (1-\varpi t)}\right)^{\frac{1}{2}}$$
$$= -\frac{c}{1-\varpi t} f'$$

Continuity equation:

$$\frac{\partial u}{\partial x} + \frac{\partial v}{\partial y} = \left(\frac{c}{1-\varpi t} f'\right) + \left(-\frac{c}{1-\varpi t} f'\right) = 0 \qquad (1.31)$$

Thus, the continuity equation (1.18) is satisfied.

$$\frac{\partial u}{\partial t}=\frac{\partial}{\partial t}\left(\frac{c}{1-\varpi t}xf'(\eta)\right),\text{ where }\eta=\left(\frac{c}{\nu_f(1-\varpi t)}\right)^{\frac{1}{2}}y$$

$$\frac{\partial u}{\partial t}=xc\frac{\partial}{\partial t}\left((1-\varpi t)^{-1}f'\right)$$

Let $a=(1-\varpi t)^{-1}$ and $b=f'(\eta)$ where $\eta=\left(\frac{c}{\nu_f(1-\varpi t)}\right)^{\frac{1}{2}}y$

$$\frac{\partial u}{\partial t}=xc\left[ab'+a'b\right]$$

$$=xc\left[(1-\varpi t)^{-1}f''\frac{\partial}{\partial t}\left(\left(\frac{c}{\nu_f(1-\varpi t)}\right)^{\frac{1}{2}}y\right)-(1-\varpi t)^{-2}(-\varpi)f'\right]$$

$$=xc\left[(1-\varpi t)^{-1}f''\left(\frac{c}{\nu_f}\right)^{\frac{1}{2}}y\frac{\partial}{\partial t}\left((1-\varpi t)^{-\frac{1}{2}}\right)-(1-\varpi t)^{-2}(-\varpi)f'\right]$$

$$=xc\left[(1-\varpi t)^{-1}f''\left(\frac{c}{\nu_f}\right)^{\frac{1}{2}}y(-\varpi)\left(-\frac{1}{2}\right)(1-\varpi t)^{-\frac{3}{2}}-(1-\varpi t)^{-2}(-\varpi)f'\right] \quad (1.32)$$

$$=\frac{1}{2}\frac{\varpi c}{(1-\varpi t)(1-\varpi t)^{\frac{3}{2}}}xf''\left(\frac{c}{\nu_f}\right)^{\frac{1}{2}}y+\frac{\varpi c}{(1-\varpi t)^2}xf'$$

$$=\frac{1}{2}\eta\frac{\varpi c}{(1-\varpi t)^2}xf''+\frac{\varpi c}{(1-\varpi t)^2}xf'$$

Apply chain rule:

$$\frac{\partial u}{\partial y}=\frac{\partial}{\partial y}\left(\frac{c}{1-\varpi t}xf'\right)$$

$$=\frac{c}{1-\varpi t}x\frac{\partial}{\partial y}\left(f'\right)\frac{\partial\eta}{\partial\eta}$$

$$=\frac{c}{1-\varpi t}x\frac{\partial}{\partial\eta}\left(f'\right)\frac{\partial\eta}{\partial y} \quad (1.33)$$

$$=\frac{c}{1-\varpi t}xf''\frac{\partial}{\partial y}\left(\sqrt{\frac{c}{\nu_f(1-\varpi t)}}y\right)$$

$$=\frac{c}{1-\varpi t}\left(\frac{c}{\nu_f(1-\varpi t)}\right)^{\frac{1}{2}}xf''$$

$$\frac{\partial^2 u}{\partial y^2} = \frac{\partial}{\partial y}\left(\frac{c}{1-\varpi t}\left(\frac{c}{\nu_f(1-\varpi t)}\right)^{\frac{1}{2}} xf''\right)$$

$$= \frac{c}{1-\varpi t}\left(\frac{c}{\nu_f(1-\varpi t)}\right)^{\frac{1}{2}} x\frac{\partial}{\partial y}\left(f''\right)\left(\frac{\partial \eta}{\partial \eta}\right)$$

$$= \frac{c}{1-\varpi t}\left(\frac{c}{\nu_f(1-\varpi t)}\right)^{\frac{1}{2}} x\frac{\partial}{\partial \eta}\left(f''\right)\left(\frac{\partial \eta}{\partial y}\right) \qquad (1.34)$$

$$= \frac{c}{1-\varpi t}\left(\frac{c}{\nu_f(1-\varpi t)}\right)^{\frac{1}{2}} xf'''\left(\frac{c}{\nu_f(1-\varpi t)}\right)^{\frac{1}{2}}$$

$$= \frac{c}{1-\varpi t}\left(\frac{c}{\nu_f(1-\varpi t)}\right) xf'''$$

$$T = T_\infty + \theta(\eta)(T_w - T_\infty)$$

$$= T_\infty + \theta\left(T_\infty + \frac{cx}{\left(1-\varpi t\right)^2} - T_\infty\right) \quad (1.35)$$

$$= T_\infty + \theta\left(\frac{cx}{\left(1-\varpi t\right)^2}\right)$$

$$\frac{\partial T}{\partial x} = \frac{\partial}{\partial x}\left[T_\infty + \theta(\eta)(T_w - T_\infty)\right]$$

$$= \frac{\partial}{\partial x}\left[T_\infty + \theta\frac{xc}{\left(1-\varpi t\right)^2}\right] \qquad (1.36)$$

$$= \frac{c}{\left(1-\varpi t\right)^2}\theta$$

$$\frac{\partial T}{\partial y} = \frac{\partial}{\partial y}\left[T_\infty + \theta(\eta)(T_w - T_\infty)\right]$$

$$= (T_w - T_\infty)\frac{d\theta}{d\eta}\frac{d\eta}{dy}$$

$$= (T_w - T_\infty)\left(\frac{c}{\nu_f(1-\varpi t)}\right)^{\frac{1}{2}}\theta' \qquad (1.37)$$

$$= \left(\frac{xc}{(1-\varpi t)^2}\right)\left(\frac{c}{\nu_f(1-\varpi t)}\right)^{\frac{1}{2}}\theta'$$

$$\frac{\partial^2 T}{\partial y^2} = \frac{\partial}{\partial y}\left[(T_w - T_\infty)\left(\frac{c}{\nu_f(1-\varpi t)}\right)^{\frac{1}{2}}\theta'\right]$$

$$= (T_w - T_\infty)\left(\frac{c}{\nu_f(1-\varpi t)}\right)^{\frac{1}{2}}\frac{\partial}{\partial \eta}\left[\theta'\right]\frac{\partial \eta}{\partial y} \qquad (1.38)$$

$$= (T_w - T_\infty)\left(\frac{c}{\nu_f(1-\varpi t)}\right)^{\frac{1}{2}}\theta''\left(\frac{c}{\nu_f(1-\varpi t)}\right)^{\frac{1}{2}}$$

$$= \frac{xc}{(1-\varpi t)^2}\left(\frac{c}{\nu_f(1-\varpi t)}\right)\theta''$$

$$\frac{\partial T}{\partial t}=\frac{\partial}{\partial t}\left[T_{\infty}+\theta(T_{w}-T_{\infty})\right]$$

$$=0+\frac{\partial}{\partial t}\left[\theta(T_{w}-T_{\infty})\right]$$

$$=\frac{\partial}{\partial t}\left[(T_{w}-T_{\infty})\right]\theta+\frac{\partial}{\partial t}\left[\theta\right](T_{w}-T_{\infty})$$

$$=\frac{\partial}{\partial t}\left(\left(T_{\infty}+\frac{xc}{\left(1-\varpi t\right)^{2}}\right)-T_{\infty}\right)\theta+\frac{\partial}{\partial \eta}\left[\theta\right]\left(\frac{\partial \eta}{\partial t}\right)\left(\left(T_{\infty}+\frac{xc}{\left(1-\varpi t\right)^{2}}\right)-T_{\infty}\right)$$

$$=\frac{\partial}{\partial t}\left(\frac{xc}{\left(1-\varpi t\right)^{2}}\right)\theta(\eta)+\frac{\partial}{\partial \eta}\left[\theta\right]\left(\frac{\partial \eta}{\partial t}\right)\left(\frac{xc}{\left(1-\varpi t\right)^{2}}\right)$$

$$=\frac{\partial}{\partial t}\left(\frac{xc}{\left(1-\varpi t\right)^{2}}\right)\theta+\frac{\partial}{\partial t}\left(\left(\frac{c}{\nu_{f}(1-\varpi t)}\right)^{\frac{1}{2}}y\right)\left(\frac{xc}{\left(1-\varpi t\right)^{2}}\right)\theta'$$

$$=\frac{\partial}{\partial t}\left(1-\varpi t\right)^{-2}xc\theta+\frac{\partial}{\partial t}\left(\left(1-\varpi t\right)^{-\frac{1}{2}}\right)\left(\frac{c}{\nu_{f}}\right)^{\frac{1}{2}}y\left(\frac{xc}{\left(1-\varpi t\right)^{2}}\right)\theta'$$

$$=\left(-2\right)\left(-\varpi\right)\left(1-\varpi t\right)^{-3}xc\theta+\frac{\varpi}{2}\left(1-\varpi t\right)^{-\frac{3}{2}}\left(\frac{c}{\nu_{f}}\right)^{\frac{1}{2}}y\left(\frac{xc}{\left(1-\varpi t\right)^{2}}\right)\theta' \qquad (1.39)$$

$$=\frac{2\varpi xc}{\left(1-\varpi t\right)^{3}}\theta+\frac{\varpi}{2\left(1-\varpi t\right)}\left(\frac{xc}{\left(1-\varpi t\right)^{2}}\right)\left(\frac{c}{\nu_{f}\left(1-\varpi t\right)}\right)^{\frac{1}{2}}y\theta'$$

$$=\frac{2\varpi xc}{\left(1-\varpi t\right)^{3}}\theta+\frac{\varpi}{2\left(1-\varpi t\right)}\left(\frac{xc}{\left(1-\varpi t\right)^{2}}\right)\eta\theta'$$

$$
\begin{aligned}
q_r &= -\frac{4\sigma^*}{3k^*}\frac{\partial T^4}{\partial y} \\
&= -\frac{4\sigma^*}{3k^*}\frac{\partial}{\partial y}\left[4T_\infty^3 T - 3T_\infty^4\right] \\
&= -\frac{4\sigma^*}{3k^*}\frac{\partial}{\partial y}\left[4T_\infty^3 T\right] \\
&= -\frac{16\sigma^* T_\infty^3}{3k^*}\frac{\partial T}{\partial y} \\
&= -\frac{16\sigma^* T_\infty^3}{3k^*}\left((T_w - T_\infty)\left(\frac{c}{\nu_f(1-\varpi t)}\right)^{\frac{1}{2}}\theta'\right) \\
&= -\frac{16\sigma^* T_\infty^3}{3k^*}\left(\frac{xc}{(1-\varpi t)^2}\left(\frac{c}{\nu_f(1-\varpi t)}\right)^{\frac{1}{2}}\theta'\right)
\end{aligned}
\tag{1.40}
$$

$$
\begin{aligned}
\frac{\partial q_r}{\partial y} &= \frac{\partial}{\partial y}\left(-\frac{16\sigma^* T_\infty^3}{3k^*}\left(\frac{xc}{(1-\varpi t)^2}\left(\frac{c}{\nu_f(1-\varpi t)}\right)^{\frac{1}{2}}\theta'\right)\right) \\
&= -\frac{16\sigma^* T_\infty^3}{3k^*}\left(\frac{xc}{(1-\varpi t)^2}\left(\frac{c}{\nu_f(1-\varpi t)}\right)^{\frac{1}{2}}\right)\frac{\partial}{\partial y}(\theta')\left(\frac{\partial \eta}{\partial \eta}\right) \\
&= -\frac{16\sigma^* T_\infty^3}{3k^*}\left(\frac{xc}{(1-\varpi t)^2}\left(\frac{c}{\nu_f(1-\varpi t)}\right)^{\frac{1}{2}}\right)\frac{\partial}{\partial \eta}(\theta')\left(\frac{\partial \eta}{\partial y}\right) \\
&= -\frac{16\sigma^* T_\infty^3}{3k^*}\left(\frac{xc}{(1-\varpi t)^2}\left(\frac{c}{\nu_f(1-\varpi t)}\right)^{\frac{1}{2}}\right)\theta''\left(\frac{c}{\nu_f(1-\varpi t)}\right)^{\frac{1}{2}} \\
&= -\frac{16\sigma^* T_\infty^3}{3k^*}\left(\frac{xc}{(1-\varpi t)^2}\left(\frac{c}{\nu_f(1-\varpi t)}\right)\right)\theta''
\end{aligned}
\tag{1.41}
$$

Substitutes into the momentum equation (1.19):

$$
\begin{aligned}
&\left(\frac{1}{2}\eta\frac{\varpi c}{\left(1-\varpi t\right)^{2}}xf''+\frac{\varpi c}{\left(1-\varpi t\right)^{2}}xf'\right)\\
&+\left(\frac{c}{1-\varpi t}xf'\right)\left(\frac{c}{1-\varpi t}f'\right)\\
&+\left(-\left(\frac{\nu_f c}{1-\varpi t}\right)^{\frac{1}{2}}f\right)\left(\frac{c}{1-\varpi t}\left(\frac{c}{\nu_f(1-\varpi t)}\right)^{\frac{1}{2}}xf''\right)\\
&=\left(\nu_{hnf}+\frac{1}{\rho_{hnf}\beta\varsigma}\right)\left(\frac{c}{1-\varpi t}\left(\frac{c}{\nu_f(1-\varpi t)}\right)xf'''\right)\\
&-\frac{1}{2\beta\varsigma^{3}\rho_{hnf}}\left(\frac{c}{1-\varpi t}\left(\frac{c}{\nu_f(1-\varpi t)}\right)^{\frac{1}{2}}xf''\right)^{2}\\
&\left(\frac{c}{1-\varpi t}\left(\frac{c}{\nu_f(1-\varpi t)}\right)xf'''\right)\\
&-\frac{\sigma_{\mathrm{hnf}}\left(B_0\left(\frac{1}{1-\varpi t}\right)^{\frac{1}{2}}\right)^{2}}{\rho_{\mathrm{hnf}}}\left(\frac{c}{1-\varpi t}xf'\right)\\
&+g\beta_{hnf}\left(\left(T_\infty+\theta\left(\frac{cx}{\left(1-\varpi t\right)^{2}}\right)\right)-T_\infty\right)\cos\alpha
\end{aligned}
\tag{1.42}
$$

Simplify (1.42) by expanding, rearranging, and expressing all terms explicitly in powers of x and derivatives of f.

$$
\begin{aligned}
&\frac{1}{2}\eta\frac{\varpi c}{\left(1-\varpi t\right)^2}xf''+\frac{\varpi c}{\left(1-\varpi t\right)^2}xf'\\
&+\left(\frac{c}{1-\varpi t}\right)^2 xf'^2\\
&-\left(\frac{c}{1-\varpi t}\right)^2 xff''\\
&=\left(\nu_{hnf}+\frac{1}{\rho_{hnf}\beta\varsigma}\right)\left(\left(\frac{c}{(1-\varpi t)}\right)^2\frac{1}{\nu_f}\right)xf'''\\
&-\frac{1}{2\beta\varsigma^3\rho_{hnf}}\left(\frac{c}{1-\varpi t}\right)^5\left(\frac{1}{\nu_f}\right)^2 x^3 f''^2 f'''\\
&-\frac{\sigma_{\mathrm{hnf}}\left(B_0\left(\frac{1}{1-\varpi t}\right)^{\frac{1}{2}}\right)^2}{\rho_{\mathrm{hnf}}}\left(\frac{c}{1-\varpi t}\right)xf'+g\beta_{hnf}\theta\left(\frac{cx}{\left(1-\varpi t\right)^2}\right)\cos\alpha
\end{aligned}
\tag{1.43}
$$

Rearrange all terms in (1.43) to one side of the equation and setting the expression equal to zero.

$$
\begin{aligned}
&\frac{1}{2\beta\varsigma^3\rho_{hnf}}\left(\frac{c}{1-\varpi t}\right)^5\left(\frac{1}{\nu_f}\right)^2 x^3 f''^2 f'''\\
&-\left(\nu_{hnf}+\frac{1}{\rho_{hnf}\beta\varsigma}\right)\left(\left(\frac{c}{(1-\varpi t)}\right)^2\frac{1}{\nu_f}\right)xf'''\\
&-\left(\frac{c}{1-\varpi t}\right)^2 xff''+\left(\frac{c}{1-\varpi t}\right)^2 xf'^2\\
&+\frac{\varpi c}{\left(1-\varpi t\right)^2}xf'+\frac{1}{2}\eta\frac{\varpi c}{\left(1-\varpi t\right)^2}xf''\\
&+\frac{\sigma_{\mathrm{hnf}}\left(B_0\left(\frac{1}{1-\varpi t}\right)^{\frac{1}{2}}\right)^2}{\rho_{\mathrm{hnf}}}\left(\frac{c}{1-\varpi t}\right)xf'-g\beta_{hnf}\theta\left(\frac{cx}{\left(1-\varpi t\right)^2}\right)\cos\alpha\\
&=0
\end{aligned}
\tag{1.44}
$$

Equation (1.44) is simplified by grouping like terms, particularly combining the third-order derivative terms and reorganizing the expression

$$\left(\frac{1}{2\beta\varsigma^3\rho_{hnf}}\left(\frac{c}{1-\varpi t}\right)^5\left(\frac{1}{\nu_f}\right)^2 x^3 f''^2-\left(\nu_{hnf}+\frac{1}{\rho_{hnf}\beta\varsigma}\right)\left(\frac{c}{1-\varpi t}\right)^2\frac{1}{\nu_f}x\right)f'''$$
$$-\left(\frac{c}{1-\varpi t}\right)^2 xff''+\left(\frac{c}{1-\varpi t}\right)^2 xf'^2$$
$$+\frac{\varpi c}{(1-\varpi t)^2}xf'+\frac{1}{2}\eta\frac{\varpi c}{(1-\varpi t)^2}xf''$$
$$+\frac{\sigma_{\text{hnf}}\left(B_0\left(\frac{1}{1-\varpi t}\right)^{\frac{1}{2}}\right)^2}{\rho_{\text{hnf}}}\left(\frac{c}{1-\varpi t}\right)xf'-g\beta_{hnf}\theta\left(\frac{cx}{(1-\varpi t)^2}\right)\cos\alpha$$
$$=0$$
(1.45)

Divides all of the term in (1.45) with $\left(\frac{c}{1-\varpi t}\right)^2 x$

$$\left(\frac{1}{2\beta\varsigma^3\rho_{hnf}}\left(\frac{c}{1-\varpi t}\right)^3\left(\frac{1}{\nu_f}\right)^2 x^2 f''^2-\left(\nu_{hnf}+\frac{1}{\rho_{hnf}\beta\varsigma}\right)\frac{1}{\nu_f}\right)f'''$$
$$-ff''+f'^2$$
$$+\frac{\varpi}{c}f'+\frac{1}{2}\eta\frac{\varpi}{c}f''$$
$$+\frac{\sigma_{\text{hnf}}\left(B_0\left(\frac{1}{1-\varpi t}\right)^{\frac{1}{2}}\right)^2}{\rho_{\text{hnf}}}\left(\frac{1-\varpi t}{c}\right)f'-g\beta_{hnf}\theta\left(\frac{1}{c}\right)\cos\alpha$$
$$=0$$
(1.46)

Let

$$\beta=\frac{\beta_0(1-\varpi t)^{\frac{3}{2}}}{x},\ \varsigma=\frac{x\varsigma_0}{(1-\varpi t)^{\frac{3}{2}}}\quad(1.47)$$

$$\beta\varsigma = \left(\frac{\beta_0\left(1-\varpi t\right)^{\frac{3}{2}}}{x}\right)\left(\frac{x\varsigma_0}{\left(1-\varpi t\right)^{\frac{3}{2}}}\right) = \beta_0\varsigma_0$$

and

$$\frac{1}{\beta\varsigma^3}\left(\frac{1}{1-\varpi t}\right)^3 x^2$$

$$= \frac{1}{\beta_0\varsigma_0\left(\frac{x\varsigma_0}{\left(1-\varpi t\right)^{\frac{3}{2}}}\right)^2}\left(\frac{1}{1-\varpi t}\right)^3 x^2$$

$$= \frac{1}{\beta_0\varsigma_0}\frac{\left(1-\varpi t\right)^3}{x^2\varsigma_0^2}\left(\frac{1}{1-\varpi t}\right)^3 x^2$$

$$= \frac{1}{\beta_0\varsigma_0}\frac{1}{\varsigma_0^2} = \frac{1}{\beta_0\varsigma_0^3}$$

$$\left(\frac{c^3}{2\beta_0\varsigma_0^3\rho_{hnf}}\left(\frac{1}{\nu_f}\right)^2 f'''^2 - \left(\nu_{hnf} + \frac{1}{\rho_{hnf}\beta_0\varsigma_0}\right)\frac{1}{\nu_f}\right) f'''$$
$$- ff'' + f'^2$$
$$+ \frac{\varpi}{c} f' + \frac{1}{2}\eta\frac{\varpi}{c} f'' \qquad (1.48)$$
$$+ \frac{\sigma_{\text{hnf}}\left(B_0\left(\frac{1}{1-\varpi t}\right)^{\frac{1}{2}}\right)^2}{\rho_{\text{hnf}}}\frac{\left(1-\varpi t\right)}{c} f' - g\beta_{hnf}\theta\left(\frac{1}{c}\right)\cos\alpha$$
$$= 0$$

Let $\nu_f = \frac{\mu_f}{\rho_f}$ and $\nu_{hnf} = \frac{\mu_{hnf}}{\rho_{hnf}}$

$$\left(\frac{c^3}{2\beta_0\varsigma_0^3\rho_{hnf}}\left(\frac{1}{\nu_f}\right)\left(\frac{\rho_f}{\mu_f}\right)f''^2-\left(\left(\frac{\mu_{hnf}}{\rho_{hnf}}\right)+\frac{1}{\rho_{hnf}\beta_0\varsigma_0}\right)\frac{\rho_f}{\mu_f}\right)f'''$$
$$-ff''+f'^2$$
$$+\frac{\varpi}{c}f'+\frac{1}{2}\eta\frac{\varpi}{c}f'' \qquad (1.49)$$
$$+\frac{\sigma_{\mathrm{hnf}}\left(B_0\left(\frac{1}{1-\varpi t}\right)^{\frac{1}{2}}\right)^2}{\rho_{\mathrm{hnf}}}\frac{(1-\varpi t)}{c}f'-g\beta_{hnf}\theta\left(\frac{1}{c}\right)\cos\alpha$$
$$=0$$

Reformulate (1.49) by factoring and rearranging terms to explicitly identify physical parameters, simplifying the equation into a dimensionless form suitable for physical interpretation.

$$\left(\frac{c^3}{2\varsigma_0^2\nu_f}\left(\frac{1}{\mu_f\beta_0\varsigma_0}\right)\frac{\rho_f}{\rho_{hnf}}f''^2-\left(\frac{\mu_{hnf}}{\mu_f}+\frac{1}{\mu_f\beta_0\varsigma_0}\right)\frac{\rho_f}{\rho_{hnf}}\right)f'''$$
$$-ff''+f'^2$$
$$+\frac{\varpi}{c}f'+\frac{1}{2}\eta\frac{\varpi}{c}f'' \qquad (1.50)$$
$$+\frac{\sigma_{\mathrm{hnf}}B_0^2}{\rho_{\mathrm{hnf}}}f'-\left(\frac{g\beta_f}{c}\right)\left(\frac{\beta_{hnf}}{\beta_f}\right)\theta\cos\alpha$$
$$=0$$

Divide (1.50) with $\frac{\rho_f}{\rho_{hnf}}$

$$\left(\frac{c^3}{2\varsigma_0^2\nu_f}\left(\frac{1}{\mu_f\beta_0\varsigma_0}\right)f''^2-\left(\frac{\mu_{hnf}}{\mu_f}+\frac{1}{\mu_f\beta_0\varsigma_0}\right)\right)f'''$$
$$-\frac{\rho_{hnf}}{\rho_f}ff''+\frac{\rho_{hnf}}{\rho_f}f'^2$$
$$+\frac{\varpi}{c}\frac{\rho_{hnf}}{\rho_f}f'+\frac{1}{2}\eta\frac{\varpi}{c}\frac{\rho_{hnf}}{\rho_f}f'' \qquad (1.51)$$
$$+\frac{\sigma_{\mathrm{hnf}}B_0^2}{\rho_f}\left(\frac{\sigma_{\mathrm{f}}}{\sigma_{\mathrm{f}}}\right)f'-\left(\frac{g\beta_f}{c}\right)\left(\frac{\beta_{hnf}}{\beta_f}\right)\frac{\rho_{hnf}}{\rho_f}\theta\cos\alpha$$
$$=0$$

The ODE for the momentum equation:

$$\begin{aligned}&\left(\omega\left(\Delta f''^{2}-1\right)-\phi_{\mu}\right) f''' \\ &+\phi_{\rho}\left(f'^{2}- ff''+A\left(f'+\frac{\eta}{2} f''\right)-\phi_{\beta}\lambda\theta\cos\alpha\right) \\ &+\phi_{\sigma}Mf' \\ &=0\end{aligned} \tag{1.52}$$

$$\Delta=\frac{c^{3}}{2\varsigma_{0}^{2}\nu_{f}},\omega=\frac{1}{\mu_{f}\beta_{0}\varsigma_{0}},A=\frac{\varpi}{c},M=\frac{\sigma_{\mathrm{f}}B_{0}^{2}}{\rho_{\mathrm{f}}c},\lambda=\frac{g\beta_{f}}{c}=\frac{Gr}{\mathrm{Re}_{x}^{2}}$$

$$\phi_{\mu}=\frac{\mu_{hnf}}{\mu_{f}},\phi_{\rho}=\frac{\rho_{hnf}}{\rho_{f}},\phi_{\beta}=\frac{\beta_{hnf}}{\beta_{f}},\phi_{\sigma}=\frac{\sigma_{hnf}}{\sigma_{f}}$$

// Don’t use phi (nano particle volume friction)

Substitutes into the energy equation (1.20):

$$\begin{aligned}&\left(\frac{2\varpi xc}{\left(1-\varpi t\right)^{3}}\theta+\frac{\varpi}{2\left(1-\varpi t\right)}\left(\frac{xc}{\left(1-\varpi t\right)^{2}}\right)\eta\theta'\right) \\ &+\left(\frac{c}{1-\varpi t}xf'\right)\left(\frac{c}{\left(1-\omega t\right)^{2}}\theta\right) \\ &+\left(-\left(\frac{\nu_{f}c}{1-\varpi t}\right)^{\frac{1}{2}}f\right)\left(\left(\frac{xc}{\left(1-\varpi t\right)^{2}}\right)\left(\frac{c}{\nu_{f}\left(1-\varpi t\right)}\right)^{\frac{1}{2}}\theta'\right) \\ &=\frac{k_{\mathrm{hnf}}}{\left(\rho C_{p}\right)_{\mathrm{hnf}}}\left[\left(\frac{xc}{\left(1-\varpi t\right)^{2}}\right)\left(\frac{c}{\nu_{f}\left(1-\varpi t\right)}\right)\theta''\right] \\ &-\frac{1}{\left(\rho C_{p}\right)_{\mathrm{hnf}}}\left[-\frac{16\sigma^{*}T_{\infty}^{3}}{3k^{*}}\left(\left(\frac{xc}{\left(1-\varpi t\right)^{2}}\right)\left(\frac{c}{\nu_{f}\left(1-\varpi t\right)}\right)\theta''\right)\right]\end{aligned} \tag{1.53}$$

Expend the equation (1.53)

$$\frac{2\varpi xc}{(1-\varpi t)^3}\theta+\frac{\varpi}{2(1-\varpi t)}\left(\frac{xc}{(1-\varpi t)^2}\right)\eta\theta'$$
$$+\left(\frac{c}{1-\varpi t}\right)\left(\frac{c}{(1-\varpi t)^2}\right)xf'\theta$$
$$-\left(\frac{c}{(1-\varpi t)^2}\right)\left(\frac{\nu_f c}{1-\varpi t}\right)^{\frac{1}{2}}\left(\frac{c}{\nu_f(1-\varpi t)}\right)^{\frac{1}{2}}xf\theta' \qquad (1.54)$$
$$=\left(\frac{xc}{(1-\varpi t)^2}\right)\frac{k_{\text{hnf}}}{(\rho C_p)_{\text{hnf}}}\left(\frac{c}{\nu_f(1-\varpi t)}\right)\theta''$$
$$+\left(\frac{xc}{(1-\varpi t)^2}\right)\frac{1}{(\rho C_p)_{\text{hnf}}}\left(\frac{c}{\nu_f(1-\varpi t)}\right)\frac{16\sigma^* T_\infty^3}{3k^*}\theta''$$

Rearrange (1.54)

$$\frac{xc}{(1-\varpi t)^2}\frac{k_{\text{hnf}}}{(\rho C_p)_{\text{hnf}}}\left(\frac{c}{\nu_f(1-\varpi t)}\right)\theta''$$
$$+\frac{xc}{(1-\varpi t)^2}\frac{1}{(\rho C_p)_{\text{hnf}}}\left(\frac{c}{\nu_f(1-\varpi t)}\right)\frac{16\sigma^* T_\infty^3}{3k^*}\theta''$$
$$+\frac{c}{(1-\varpi t)^2}\left(\frac{\nu_f c}{1-\varpi t}\right)^{\frac{1}{2}}\left(\frac{c}{\nu_f(1-\varpi t)}\right)^{\frac{1}{2}}xf\theta' \qquad (1.55)$$
$$-\left(\frac{c}{1-\varpi t}\right)\left(\frac{c}{(1-\varpi t)^2}\right)xf'\theta$$
$$-\frac{2\varpi xc}{(1-\varpi t)^3}\theta$$
$$-\frac{\varpi}{2(1-\varpi t)}\left(\frac{xc}{(1-\varpi t)^2}\right)\eta\theta'=0$$

Simplify (1.55)

$$\frac{xc}{(1-\varpi t)^2}\frac{k_{\text{hnf}}}{(\rho C_p)_{\text{hnf}}}\left(\frac{c}{\nu_f(1-\varpi t)}\right)\theta''$$
$$+\frac{xc}{(1-\varpi t)^2}\frac{1}{(\rho C_p)_{\text{hnf}}}\left(\frac{c}{\nu_f(1-\varpi t)}\right)\frac{16\sigma^* T_\infty^3}{3k^*}\theta''$$
$$+\frac{c}{(1-\varpi t)^2}\left(\frac{c}{1-\varpi t}\right)xf\,\theta'$$
$$-\left(\frac{c}{(1-\varpi t)^2}\right)\left(\frac{c}{1-\varpi t}\right)xf'\theta \qquad (1.56)$$
$$-\frac{2\varpi xc}{(1-\varpi t)^3}\theta$$
$$-\frac{\varpi}{2(1-\varpi t)}\left(\frac{xc}{(1-\varpi t)^2}\right)\eta\theta' = 0$$

Divides $\frac{c^2}{(1-\varpi t)^3}x$

$$\frac{1-\varpi t}{c}\frac{k_{\text{hnf}}}{(\rho C_p)_{\text{hnf}}}\left(\frac{c}{\nu_f(1-\varpi t)}\right)\theta''$$
$$+\frac{1}{(\rho C_p)_{\text{hnf}}}\left(\frac{1}{\nu_f}\right)\frac{16\sigma^* T_\infty^3}{3k^*}\theta''$$
$$+f\,\theta' \qquad (1.57)$$
$$-f'\theta$$
$$-\frac{2\varpi}{c}\theta$$
$$-\frac{\varpi}{2(1-\varpi t)}\left(\frac{1-\varpi t}{c}\right)\eta\theta' = 0$$

Simplify

$$
\begin{aligned}
&\frac{k_{\text{hnf}}}{(\rho C_p)_{\text{hnf}}}\left(\frac{1}{\nu_f}\right)\theta'' \\
&+\frac{1}{(\rho C_p)_{\text{hnf}}}\left(\frac{1}{\nu_f}\right)\frac{16\sigma^* T_\infty^3}{3k^*}\theta'' \\
&+f\theta' \\
&-f'\theta \\
&-2\left(\frac{\varpi}{c}\right)\theta \\
&-\frac{1}{2}\left(\frac{\varpi}{c}\right)\eta\theta' = 0
\end{aligned}
\tag{1.58}
$$

Reformulate (1.58) by factoring and rearranging terms to explicitly identify physical parameters, simplifying the equation into a dimensionless form suitable for physical interpretation.

$$
\begin{aligned}
&\frac{k_{\text{f}}}{\nu_f(\rho C_p)_{\text{f}}}\left(\frac{(\rho C_p)_{\text{f}}}{(\rho C_p)_{\text{hnf}}}\right)\left(\frac{k_{\text{hnf}}}{k_{\text{f}}}\right)\theta'' \\
&+\frac{k_{\text{f}}}{\nu_f(\rho C_p)_{\text{f}}}\left(\frac{(\rho C_p)_{\text{f}}}{(\rho C_p)_{\text{hnf}}}\right)\left(\frac{4}{3}\right)\frac{4\sigma^* T_\infty^3}{k_{\text{f}}k^*}\theta'' \\
&+f\theta' \\
&-f'\theta \\
&-2\left(\frac{\varpi}{c}\right)\theta \\
&-\frac{\eta}{2}\left(\frac{\varpi}{c}\right)\theta' = 0
\end{aligned}
\tag{1.59}
$$

The 2nd order ODE for the energy equation:

$$\left(\frac{(\rho C_p)_{\mathrm{f}}}{(\rho C_p)_{\mathrm{hnf}}}\right)\left[\frac{1}{\mathrm{Pr}}\left(\left(\frac{k_{\mathrm{hnf}}}{k_{\mathrm{f}}}\right)+\left(\frac{4}{3}\right)Rd\right)\theta''\right]$$
$$-\theta f^{'}+\theta' f-A\left(2\theta+\frac{\eta}{2}\theta'\right)=0 \qquad (1.60)$$

$$\mathrm{Pr}=\frac{\nu_f(\rho C_p)_{\mathrm{f}}}{k_{\mathrm{f}}}$$
$$Rd=\frac{4\sigma^{*}T_{\infty}^{3}}{k_{\mathrm{f}}k^{*}}$$
$$A=\frac{\varpi}{c}$$

Boundary conditions at y=0, equation (1.24) implies $\eta(0)=0$:

Assuming,

$$v_w=-\left(\frac{\nu_f c}{1-\varpi t}\right)^{\frac{1}{2}}S \qquad (1.61)$$

Therefore, the boundary conditions for v is,

$$v=v_w \qquad (1.62)$$

$$-\left(\frac{\nu_f c}{1-\varpi t}\right)^{\frac{1}{2}}f(0)=-\left(\frac{\nu_f c}{1-\varpi t}\right)^{\frac{1}{2}}S \qquad (1.63)$$

$$f(0)=S \qquad (1.64)$$

Assuming,

$$\Omega=L_0\left(\frac{c}{\nu_f}\right)^{\frac{1}{2}} \qquad (1.65)$$

Therefore, the boundary conditions for u is,

$$u(x,y)=U_w+L\left[\frac{\partial u}{\partial y}\right]_{y=0} \qquad (1.66)$$

$$\frac{c}{1-\varpi t}xf'(0)=\frac{cx}{1-\varpi t}+L\left(\frac{c}{1-\varpi t}\left(\frac{c}{\nu_f(1-\varpi t)}\right)^{\frac{1}{2}}xf''(0)\right) \tag{1.67}$$

Divide by $\frac{cx}{1-\varpi t}$

$$\begin{aligned}
f'(0)&=1+L\left(\frac{c}{\nu_f(1-\varpi t)}\right)^{\frac{1}{2}}f''(0)\\
&=1+\left(L_0(1-\varpi t)^{\frac{1}{2}}\right)\left(\frac{c}{\nu_f(1-\varpi t)}\right)^{\frac{1}{2}}f''(0) \qquad (1.68)\\
&=1+L_0\left(\frac{c}{\nu_f}\right)^{\frac{1}{2}}f''(0)\\
&=1+\Omega f''(0)
\end{aligned}$$

Assuming,

$$Bi=\frac{h_f}{k_f}\left(\frac{\nu_f}{c}\right)^{\frac{1}{2}} \tag{1.69}$$

Therefore, by inserting (1.23), (1.35) and (1.37) into (1.21) , the boundary conditions for $\theta(0)$ is,

//suppose to be theta(0)

$$\begin{aligned}
&-k_f\left[\left(\frac{xc}{(1-\varpi t)^2}\right)\left(\frac{c}{\nu_f(1-\varpi t)}\right)^{\frac{1}{2}}\theta'\right] \qquad (1.70)\\
&=h_f\left(\left(T_\infty+\frac{xc}{(1-\varpi t)^2}\right)-\left(T_\infty+\theta\left(\frac{cx}{(1-\varpi t)^2}\right)\right)\right)
\end{aligned}$$

$$\theta'(0) = -\frac{h_f}{k_f}\left(\frac{\nu_f(1-\varpi t)}{c}\right)^{\frac{1}{2}}\left(1+\theta(0)\right)$$
$$= -\frac{h_f}{k_f}\left(\frac{\nu_f}{c}\right)^{\frac{1}{2}}\left(1-\theta(0)\right)$$
$$= -Bi\left(1-\theta(0)\right) \qquad (1.71)$$

$$\lim_{Bi\to\infty}\frac{\theta'}{Bi} = \theta - 1$$
$$\frac{\theta'}{\infty} = \theta - 1$$
$$0 = \theta - 1$$
$$\theta \to 1$$

Boundary conditions as $y \to \infty$, equation (1.24) implies $\eta \to \infty$.

Boundary conditions as $u \to 0$, implies,

$$\frac{c}{1-\varpi t} x f'(\infty) \to 0 \qquad (1.72)$$

$$f'(\infty) \to 0 \qquad (1.73)$$

Boundary conditions as $T \to T_\infty$, equation (1.24) implies,

$$T_\infty + \theta(\infty)(T_w - T_\infty) \to T_\infty \qquad (1.74)$$

$$\theta(\infty)(T_w - T_\infty) \to 0 \qquad (1.75)$$

$$\theta(\infty) \to 0 \qquad (1.76)$$

Reduce (1.52) and (1.60) to 1st order equation,

Let,

$y(1) = f,$

$y'(1) = y(2) = f',$

$y'(2) = y(3) = f'',$

$y(4) = \theta,$

$y'(4) = y(5) = \theta',$

$ya(1) = f(0),$

$ya(2) = f'(0),$

$ya(3) = f''(0),$

$ya(4) = \theta(0),$

$ya(5) = \theta'(0),$

$yb(1) = f(\infty)$

$yb(2) = f'(\infty)$

$yb(4) = \theta(\infty)$

$$f''' = -\left(\frac{1}{\omega\left(\Delta y_3^{\,2} - 1\right) - b_\mu}\right)\left[b_\rho\left(y_2^{\,2} - y_1 y_3 + A\left(y_2 + \frac{\eta}{2} y_3\right) - b_\beta \lambda y_4 \cos\alpha\right) + b_\sigma M y_2\right]$$

$$\theta'' = \frac{1}{\left(b_k + \left(\frac{4}{3}\right)Rd\right)}\left(\Pr b_{\rho Cp}\left(y_4 y_2 - y_5 y_1 + A\left(2y_4 + \frac{\eta}{2} y_5\right)\right) - Ec\left(b_\mu\right) y_3^{\,2}\right)$$

$$\Delta = \frac{c^3}{2\varsigma_0^2 \nu_f}, \omega = \frac{1}{\mu_f \beta_0 \varsigma_0}, A = \frac{\varpi}{c}, M = \frac{\sigma_f B_0^2}{\rho_f c}, \lambda = \frac{g\beta_f}{c},$$

$$\Pr = \frac{\nu_f (\rho C_p)_f}{k_f}, Rd = \frac{4\sigma^* T_\infty^3}{k_f k^*}, Ec = \frac{cx\mu_f}{\nu_f (\rho C_p)_f}$$

$$b_\mu = \frac{\mu_{hnf}}{\mu_f}, b_\rho = \frac{\rho_{hnf}}{\rho_f}, b_\beta = \frac{\beta_{hnf}}{\beta_f}, b_\sigma = \frac{\sigma_{hnf}}{\sigma_f}, b_{\rho Cp} = \frac{(\rho C_p)_{hnf}}{(\rho C_p)_f}, b_k = \frac{k_{hnf}}{k_f}$$

$ya(1) = S$

$ya(2) = 1 + S_l\, ya(3)$

$ya(5) = -Bi(1 - ya(4))$

$yb(2) \to 0$

$yb(4) \to 0$

(1.77)

Try to validate again

The derivation for skin friction coefficient C_f

$$C_f = \frac{\tau_w}{\rho U_w^2} \text{ where}$$

$$\tau_w = \left[\left(\mu_{hnf} + \frac{1}{\beta\varsigma} \right) \frac{\partial u}{\partial y} - \frac{1}{6\beta\varsigma^3} \left(\frac{\partial u}{\partial y} \right)^3 \right]_{y=0}$$

$$= \left(\mu_{hnf} + \frac{1}{\beta\varsigma} \right) \left(\frac{c}{1-\varpi t} \left(\frac{c}{\nu_f (1-\varpi t)} \right)^{\frac{1}{2}} xf''(0) \right) - \frac{1}{6\beta\varsigma^3} \left(\frac{c}{1-\varpi t} \left(\frac{c}{\nu_f (1-\varpi t)} \right)^{\frac{1}{2}} xf''(0) \right)^3$$

(1.78)

$$C_f = \frac{1}{\rho U_w^2}\left[\left(\mu_{hnf} + \frac{1}{\beta\varsigma}\right)\left(\frac{c}{1-\varpi t}\left(\frac{c}{\nu_f(1-\varpi t)}\right)^{\frac{1}{2}} xf''(0)\right) - \frac{1}{6\beta\varsigma^3}\left(\frac{c}{1-\varpi t}\left(\frac{c}{\nu_f(1-\varpi t)}\right)^{\frac{1}{2}} xf''(0)\right)^3\right]$$

$$= \frac{1}{\rho U_w^2}\left[\begin{array}{l}\left(\mu_{hnf}\,\frac{c}{1-\varpi t}\left(\frac{1}{\nu_f}\right)^{\frac{1}{2}}\left(\frac{c}{1-\varpi t}\right)^{\frac{1}{2}} + \frac{1}{\beta\varsigma}\frac{c}{1-\varpi t}\left(\frac{1}{\nu_f}\right)^{\frac{1}{2}}\left(\frac{c}{1-\varpi t}\right)^{\frac{1}{2}}\right) xf''(0) \\ -\frac{1}{\beta\varsigma^3}\left(\frac{1}{1-\varpi t}\right)^3 x^2\frac{1}{6}c^3\frac{c}{\nu_f(1-\varpi t)}\left(\frac{1}{\nu_f}\right)^{\frac{1}{2}}\left(\frac{c}{1-\varpi t}\right)^{\frac{1}{2}} x\left(f''(0)\right)^3\end{array}\right]$$

$$= \frac{1}{\rho U_w^2}\left(\frac{c}{1-\varpi t}\right)^{\frac{1}{2}} x\left[\begin{array}{l}\left(\mu_{hnf}\,\frac{c}{1-\varpi t}\left(\frac{1}{\nu_f}\right)^{\frac{1}{2}} + \frac{1}{\beta\varsigma}\frac{c}{1-\varpi t}\left(\frac{1}{\nu_f}\right)^{\frac{1}{2}}\right) f''(0) \\ -\frac{1}{\beta\varsigma^3}\left(\frac{1}{1-\varpi t}\right)^3 x^2\frac{1}{6}c^3\frac{1}{\nu_f}\frac{c}{(1-\varpi t)}\left(\frac{1}{\nu_f}\right)^{\frac{1}{2}}\left(f''(0)\right)^3\end{array}\right]$$

(1.79)

Let (1.47) into (1.79)

$$C_f = \frac{1}{\rho U_w^2}\left(\frac{c}{1-\varpi t}\right)^{\frac{1}{2}} x\left[\begin{array}{l}\left(\mu_{hnf}\,\frac{c}{1-\varpi t}\left(\frac{1}{\nu_f}\right)^{\frac{1}{2}} + \frac{1}{\beta_0\varsigma_0}\frac{c}{1-\varpi t}\left(\frac{1}{\nu_f}\right)^{\frac{1}{2}}\right) f''(0) \\ -\frac{1}{\beta_0\varsigma_0^3}\frac{1}{6}c^3\frac{1}{\nu_f}\frac{c}{(1-\varpi t)}\left(\frac{1}{\nu_f}\right)^{\frac{1}{2}}\left(f''(0)\right)^3\end{array}\right]$$

(1.80)

Insert U_w in (1.23) into (1.80)

$$C_f = \frac{1}{\rho\left(\frac{xc}{1-\varpi t}\right)^2}\left(\frac{c}{1-\varpi t}\right)^{\frac{1}{2}} x\begin{bmatrix}\left(\mu_{hnf}\frac{c}{1-\varpi t}\left(\frac{1}{\nu_f}\right)^{\frac{1}{2}}+\frac{1}{\beta_0\varsigma_0}\frac{c}{1-\varpi t}\left(\frac{1}{\nu_f}\right)^{\frac{1}{2}}\right)f''(0)\\ -\frac{1}{\beta_0\varsigma_0^3}\frac{1}{6}c^3\frac{1}{\nu_f}\frac{c}{(1-\varpi t)}\left(\frac{1}{\nu_f}\right)^{\frac{1}{2}}\left(f''(0)\right)^3\end{bmatrix}$$

$$= \frac{1}{\rho}\left(\frac{1-\varpi t}{xc}\right)^2\left(\frac{c}{1-\varpi t}\right)^{\frac{1}{2}} x\begin{bmatrix}\left(\mu_{hnf}\frac{c}{1-\varpi t}\left(\frac{1}{\nu_f}\right)^{\frac{1}{2}}+\frac{1}{\beta_0\varsigma_0}\frac{c}{1-\varpi t}\left(\frac{1}{\nu_f}\right)^{\frac{1}{2}}\right)f''(0)\\ -\frac{1}{\beta_0\varsigma_0^3}\frac{1}{6}c^3\frac{1}{\nu_f}\frac{c}{(1-\varpi t)}\left(\frac{1}{\nu_f}\right)^{\frac{1}{2}}\left(f''(0)\right)^3\end{bmatrix}$$

$$= \frac{1}{\rho}\left(\frac{1-\varpi t}{c}\right)^2\left(\frac{c}{1-\varpi t}\right)^{\frac{1}{2}}\frac{1}{x}\begin{bmatrix}\left(\mu_{hnf}\frac{c}{1-\varpi t}\left(\frac{\rho_f}{\mu_f}\right)^{\frac{1}{2}}+\frac{1}{\beta_0\varsigma_0}\frac{c}{1-\varpi t}\left(\frac{\rho_f}{\mu_f}\right)^{\frac{1}{2}}\right)f''(0)\\ -\frac{c^3}{2\varsigma_0^2\nu_f}\frac{1}{3}\frac{1}{\beta_0\varsigma_0}\frac{c}{(1-\varpi t)}\left(\frac{\rho_f}{\mu_f}\right)^{\frac{1}{2}}\left(f''(0)\right)^3\end{bmatrix}$$

$$= \frac{1}{\rho}\frac{1}{x}\left(\frac{1-\varpi t}{c}\right)\left(\frac{c}{1-\varpi t}\right)^{\frac{1}{2}}\left(\frac{\rho_f}{\mu_f}\right)^{\frac{1}{2}}\left(\frac{\mu_f}{\mu_f}\right)\begin{bmatrix}\left(\mu_{hnf}+\frac{1}{\beta_0\varsigma_0}\right)f''(0)\\ -\frac{c^3}{2\varsigma_0^2\nu_f}\frac{1}{3}\frac{1}{\beta_0\varsigma_0}\left(f''(0)\right)^3\end{bmatrix}$$

$$= \frac{1}{x}\left(\frac{1-\varpi t}{c}\right)\left(\frac{\mu_f}{\rho}\right)\left[\left(\frac{c}{1-\varpi t}\right)\left(\frac{\rho_f}{\mu_f}\right)\right]^{\frac{1}{2}}\begin{bmatrix}\left(\left(\frac{\mu_{hnf}}{\mu_f}\right)+\frac{1}{\mu_f\beta_0\varsigma_0}\right)f''(0)\\ -\frac{1}{3}\frac{c^3}{2\varsigma_0^2\nu_f}\frac{1}{\mu_f\beta_0\varsigma_0}\left(f''(0)\right)^3\end{bmatrix}$$

$$= \left[\frac{1}{x^2}\left(\frac{1-\varpi t}{c}\right)\left(\frac{\mu_f}{\rho}\right)\right]^{\frac{1}{2}}\begin{bmatrix}\left(\left(\frac{\mu_{hnf}}{\mu_f}\right)+\frac{1}{\mu_f\beta_0\varsigma_0}\right)f''(0)\\ -\frac{1}{3}\frac{c^3}{2\varsigma_0^2\nu_f}\frac{1}{\mu_f\beta_0\varsigma_0}\left(f''(0)\right)^3\end{bmatrix}$$

$$= \left(\frac{1}{\mathrm{Re}_x}\right)^{\frac{1}{2}}\left[\left(\phi_\mu+\omega\right)f''(0)-\frac{\Delta\omega}{3}f'^3(0)\right] \qquad (1.81)$$

Rewrite (1.81) in term of $f''(0)$

$$C_f \,\mathrm{Re}_x^{\frac{1}{2}} = \left(\phi_\mu + \omega\right) f''(0) - \frac{1}{3}\Delta\omega f'''(0) \tag{1.82}$$

// raynold number keluarkan equation.| rho Ganti dengan rhof

The derivation for Nusselt number, $\mathrm{Nu_x}$

$$Nu_x = \frac{xq_w}{k_f\left(T_w - T_\infty\right)}, \text{ where}$$

$$q_w = -k_{hnf}\left[1 + \frac{16\sigma^* T_\infty^3}{3k^* k_f}\right]\left(\frac{\partial T}{\partial y}\right)_{y=0}$$

$$= -k_{hnf}\left[1 + 4\left(\frac{4\sigma^* T_\infty^3}{3k^* k_f}\right)\right]\left(\left(\frac{xc}{\left(1-\varpi t\right)^2}\right)\left(\frac{c}{\nu_f(1-\varpi t)}\right)^{\frac{1}{2}}\theta'\right)_{y=0} \tag{1.83}$$

$$= -k_{hnf}\left[1 + 4\left(\frac{4\sigma^* T_\infty^3}{3k^* k_f}\right)\right]\left(\frac{xc}{\left(1-\varpi t\right)^2}\right)\left[\frac{c}{(1-\varpi t)}\left(\frac{\rho_f}{\mu_f}\right)\right]^{\frac{1}{2}}\theta'(0)$$

and $\left(T_w - T_\infty\right) = \dfrac{xc}{\left(1-\varpi t\right)^2}$

Hence,

$$Nu_x = \frac{x}{k_f\left(T_w - T_\infty\right)}\left(-k_{hnf}\left[1 + 4\left(\frac{4\sigma^* T_\infty^3}{3k^* k_f}\right)\right]\left(T_w - T_\infty\right)\left[\frac{c}{(1-\varpi t)}\left(\frac{\rho_f}{\mu_f}\right)\right]^{\frac{1}{2}}\theta'(0)\right)$$

$$= -\frac{k_{hnf}}{k_f}\left[1 + 4\left(\frac{4\sigma^* T_\infty^3}{3k^* k_f}\right)\right]\left[x^2\frac{c}{(1-\varpi t)}\left(\frac{\rho_f}{\mu_f}\right)\right]^{\frac{1}{2}}\theta'(0)$$

$$= -\frac{k_{hnf}}{k_f}\left[1 + 4\mathrm{Rd}\right]\mathrm{Re}_x^{\frac{1}{2}}\theta'(0)$$

(1.84)

Rewrite (1.84) in term of $\theta'(0)$

$$Nu_x \,\mathrm{Re}_x^{-\frac{1}{2}} = -\frac{k_{hnf}}{k_f}\left[1 + 4\mathrm{Rd}\right]\theta'(0) \tag{1.85}$$

// Validate selain Pr. Sekarang just dah validate energy. Perlu validate momentum. Cari juga f''. letak mana yg jumpa. Atleast 3.

// result tukar2 mhd, dan incline (3 value je biasa)

// nusselt number + Cf dalam matlab (value+graf)

// 20 August Present result and validation

// proposal: ch1+2+3. Chapter 3 letak semua problem. Chapter 4 expected result. Reference. Gant chart

APPENDIX 2

Year	2025										2026							
Months	3	4	5	6	7	8	9	10	11	12	1	2	3	4	5	6	7	8
Mathematical Modelling																		
Numerical Solution																		
Data Analysis																		
Writing Report																		

RESEARCH ACTIVITIES	START DATE	END DATE
LITERATURE REVIEW	24/3/2025	19/9/2026
RESEARCH PROPOSAL	24/3/2025	23/9/2025
RESEARCH ETHICS	23/9/2025	22/11/2025
METHODOLOGY 1	22/6/2025	21/10/2025
METHODOLOGY 2	21/10/2025	19/2/2026
METHODOLOGY 3	19/2/2026	21/6/2026
THESIS WRITING	23/9/2025	19/9/2026
THESIS EXAMINATION	19/9/2026	28/11/2026
THESIS CORRECTION	28/11/2026	26/2/2027
REGISTERED	24/3/2025	
DEFENSE RESEARCH PROPOSAL	23/9/2025	
RESEARCH ETHICS APPROVED	22/11/2025	
RESEARCH OBJECTIVE 1	21/10/2025	
RESEARCH OBJECTIVE 2	19/2/2026	
RESEARCH OBJECTIVE 3	21/6/2026	
THESIS SUBMITTED	19/9/2026	
VIVA VOCE	28/11/2026	
STUDY COMPLETED	23/3/2027	

Table 7: Project Gant Chart

AUTHOR'S PROFILE

Nur Arif Husaini Bin Norwaza obtained Bachelor of Science (Hons.) Computational Mathematics in June 2021 from Universiti Teknologi MARA. Arif's broader interests span numerical analysis, scientific computing, AI-driven optimisation, and the design of enterprise-scale web architectures. He has published in peer-reviewed journals on applied mathematics and contributes to industrial projects that integrate Laravel, Nuxt.js and PostgreSQL back ends. Passionate about knowledge transfer, he frequently mentors' junior developers and leads workshops on advanced coding patterns and data-driven problem solving.